Electronic Supplementary Material (ESI) for Physical Chemistry Chemical Physics.

Supplementary Information

Introducing Asymmetry in Tetradentate Azadipyrromethene Chromophores:

A Systematic Study of the Impact on Electronic and Photophysical Properties

*André Bessette[1,2], Mihaela Cibian[1], Francis Bélanger[2], Denis Désilets[2] and Garry S. Hanan[1] *.*

[1]Département de Chimie, Université de Montréal, Pavillon J.-A. Bombardier, 5155 Decelles Avenue, Montréal, Québec, H3T-2B1, Canada

[2] Saint-Jean Photochemicals Inc., 725 Trotter street, Saint-Jean-sur-Richelieu, Québec, J3B 8J8, Canada.

Table of Contents

NMR Characterization **3**
HRMS Characterization **10**
Electrochemistry **12**
Computational Modelization **24**
X-ray diffraction measurements and structure determination **34**
References **40**

NMR Characterization

Figure S.1 – ^{1}H of *Azadipyrromethene* **3** ($CDCl_3$; poorly soluble)

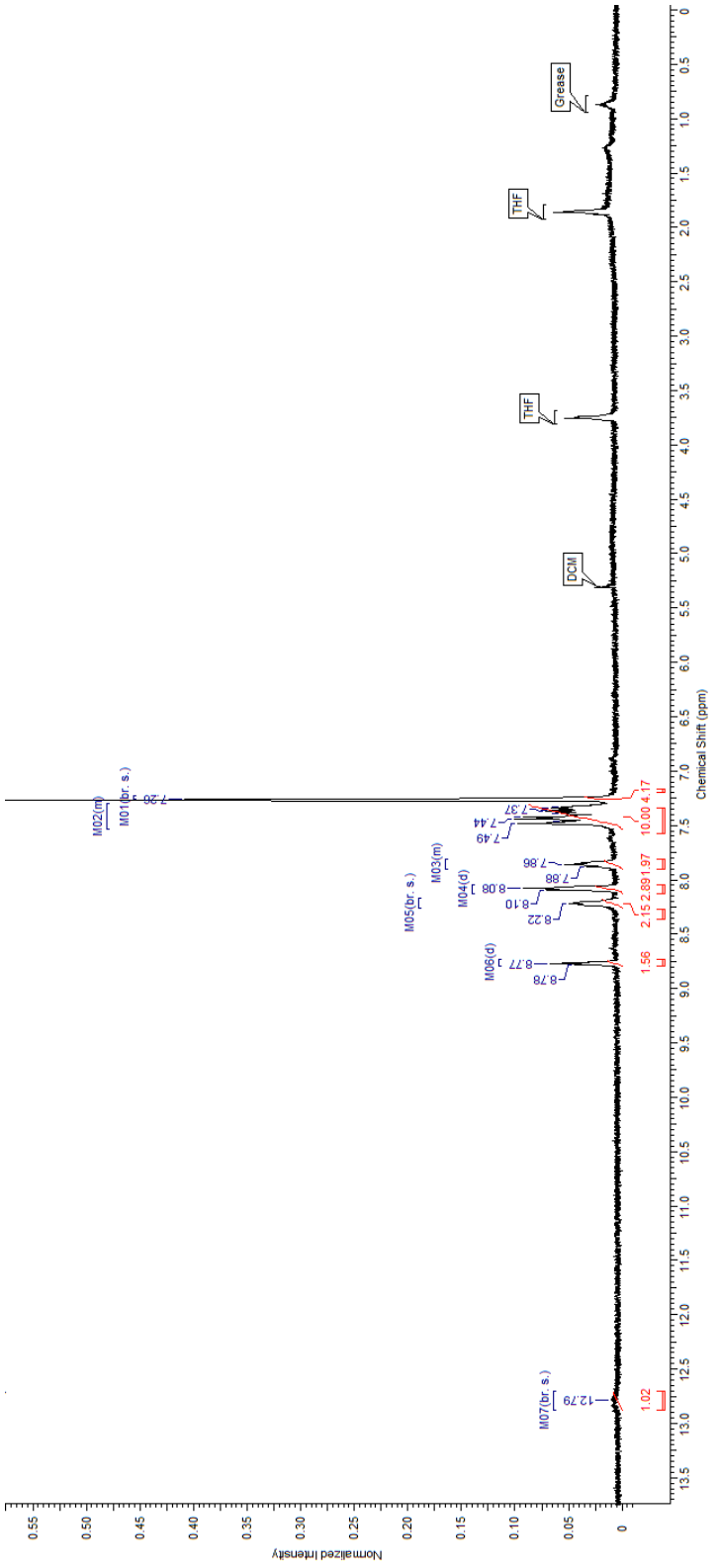

Figure S.2 – ^{1}H of *Azadipyrromethene* **4** ($CDCl_3$)

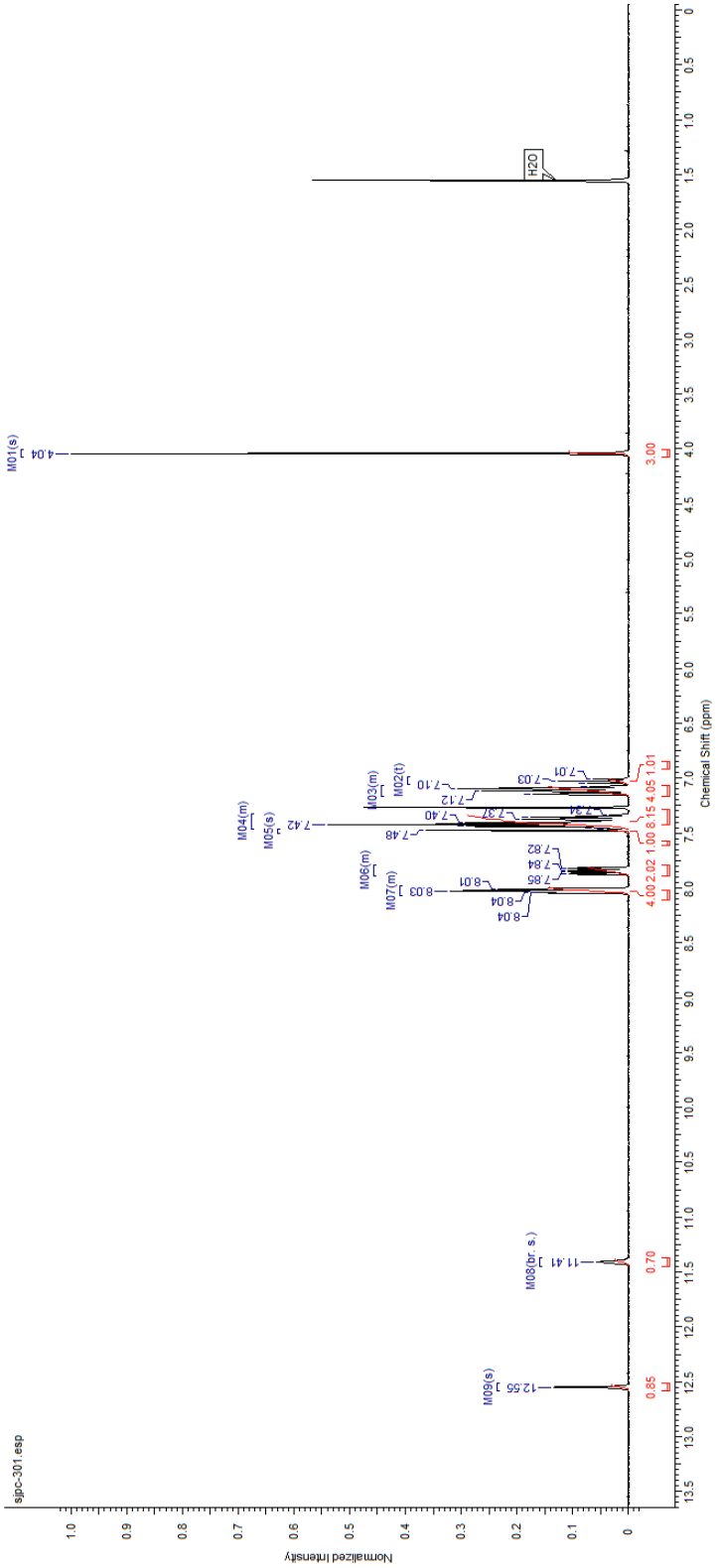

Figure S.3 – ^{13}C of *Azadipyrromethene* **4** ($CDCl_3$)

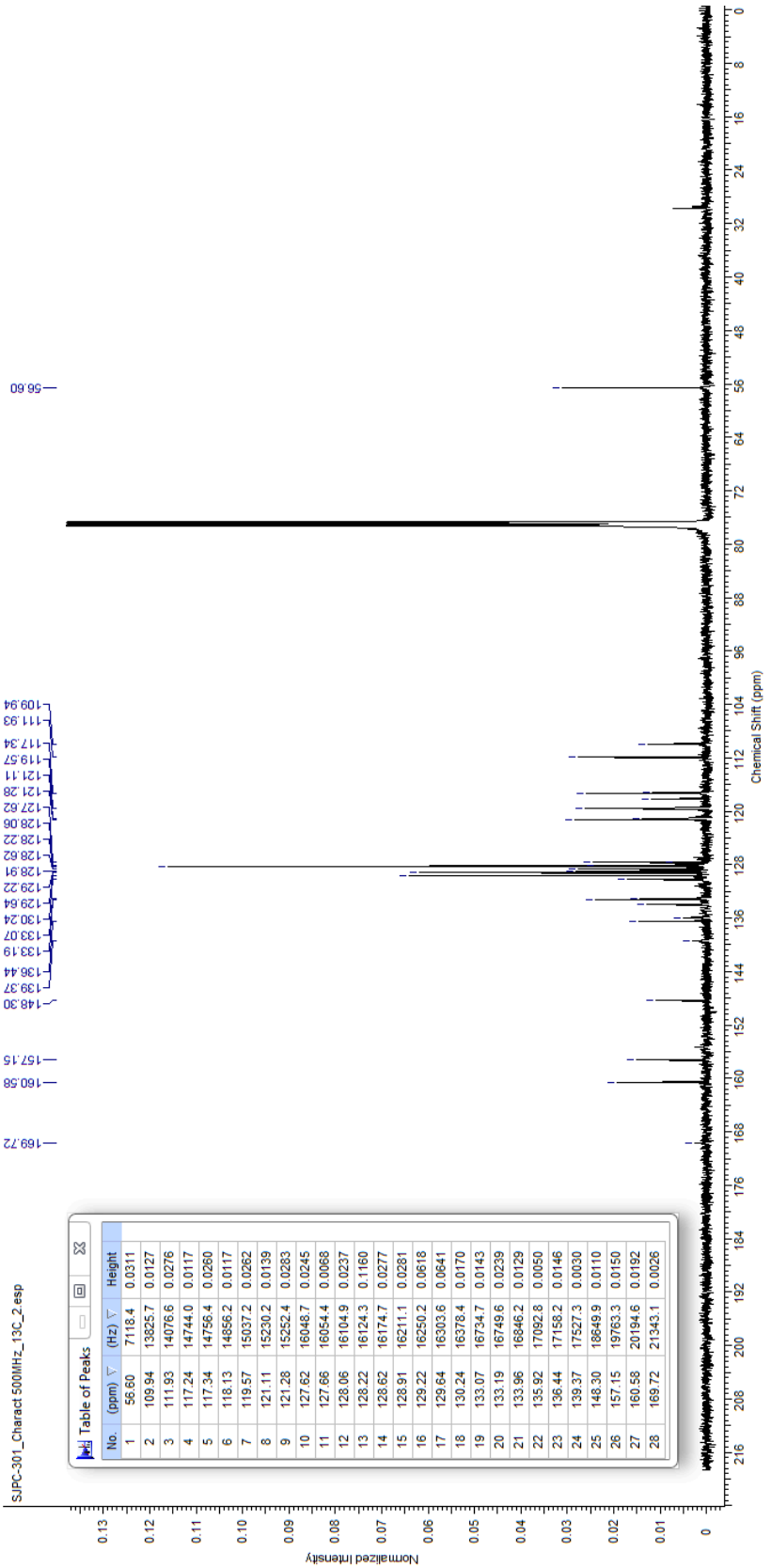

Figure S.4 – ^{1}H of *Azadipyrromethene* **5** ($CDCl_3$)

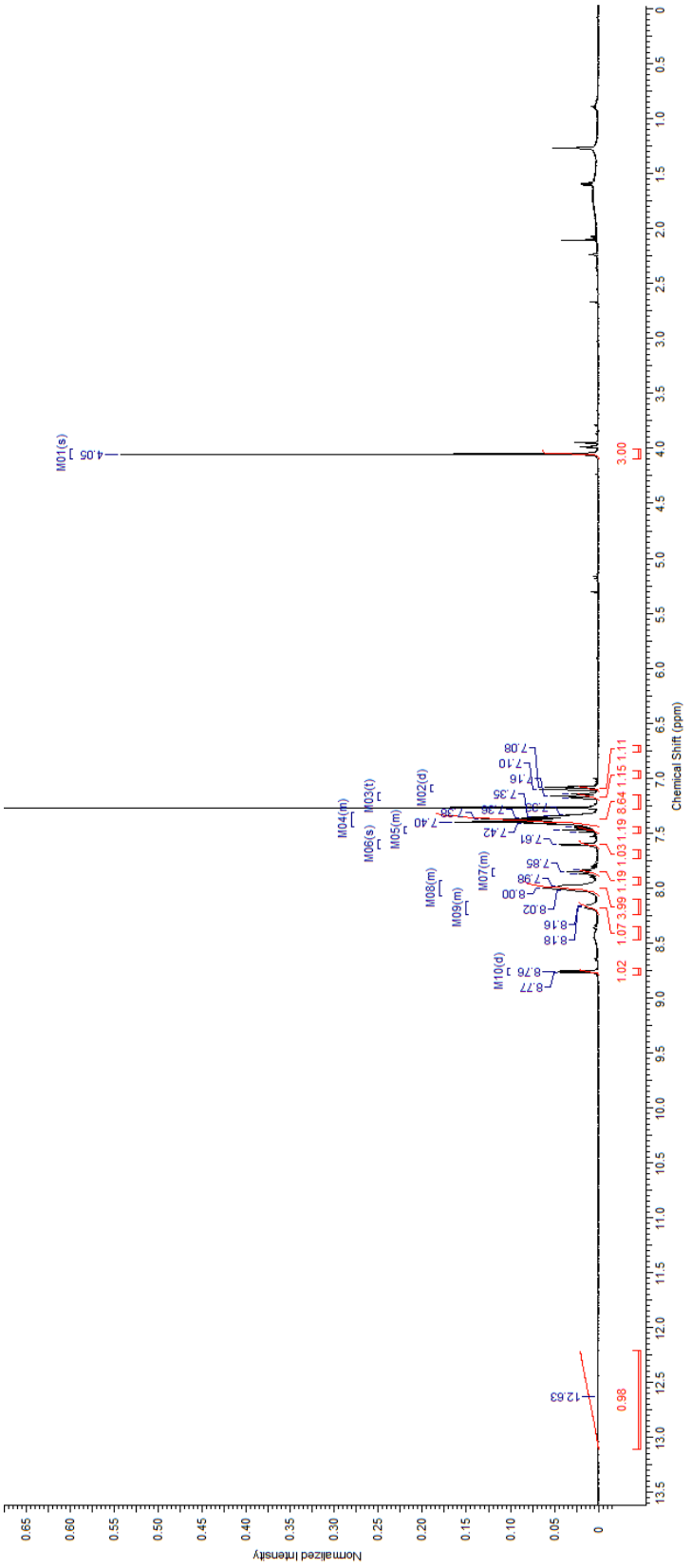

Figure S.5 – ^{13}C of *Azadipyrromethene* **5** ($CDCl_3$)

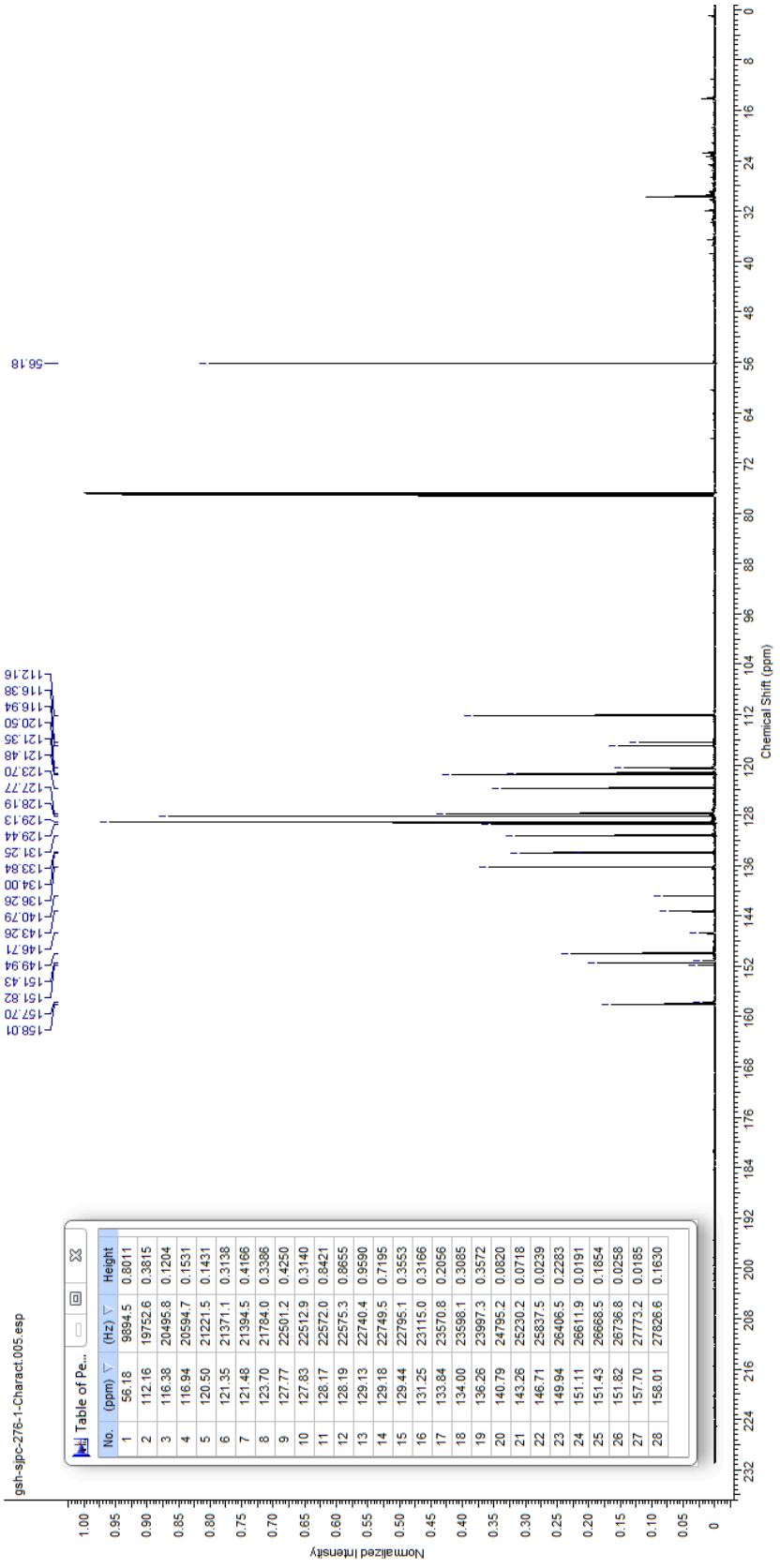

Figure S.6 – ^{1}H of *Azadipyrromethene* **6** ($CDCl_3$)

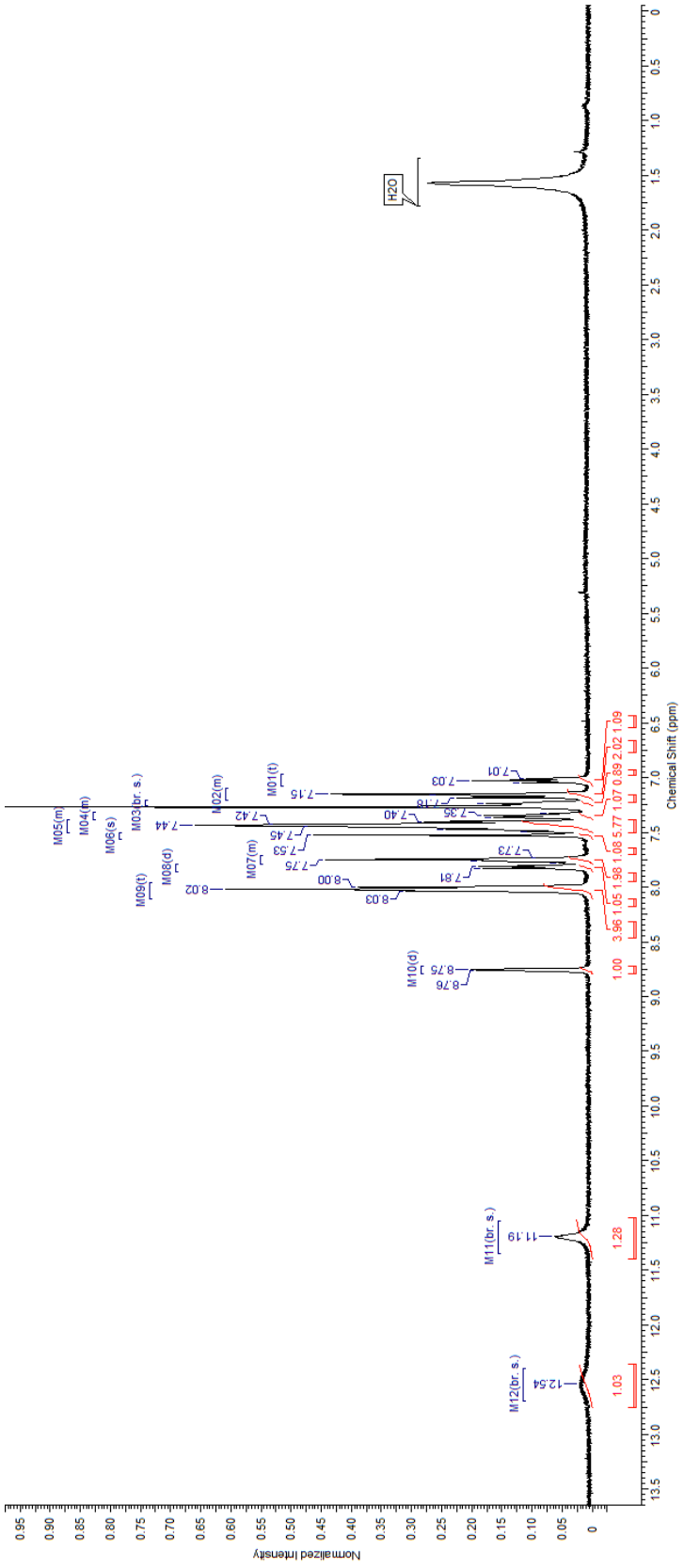

Figure S.7 – ^{13}C of *Azadipyrromethene* **6** ($CDCl_3$)

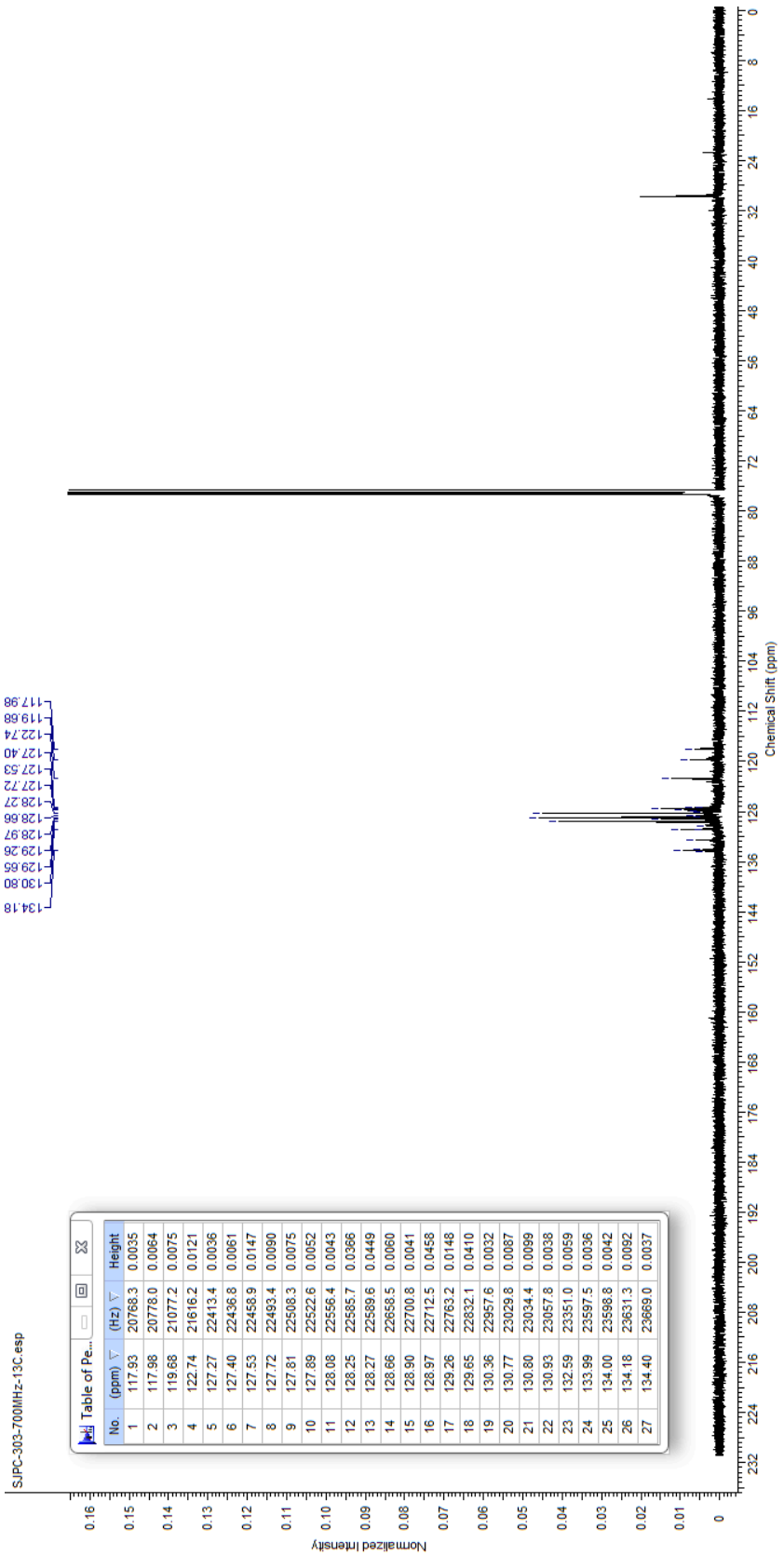

No.	(ppm)	(Hz)	Height
1	117.93	20768.3	0.0035
2	117.98	20778.0	0.0064
3	119.68	21077.2	0.0075
4	122.74	21616.2	0.0121
5	127.27	22413.4	0.0036
6	127.40	22436.8	0.0061
7	127.53	22458.9	0.0147
8	127.72	22493.4	0.0090
9	127.81	22508.3	0.0075
10	127.89	22522.6	0.0052
11	128.08	22556.4	0.0043
12	128.25	22585.7	0.0366
13	128.27	22589.6	0.0449
14	128.66	22658.5	0.0060
15	128.90	22700.8	0.0041
16	128.97	22712.5	0.0458
17	129.26	22763.2	0.0148
18	129.65	22832.1	0.0410
19	130.36	22957.6	0.0032
20	130.77	23029.8	0.0087
21	130.80	23034.4	0.0099
22	130.93	23057.8	0.0038
23	132.59	23351.0	0.0059
24	133.99	23597.5	0.0036
25	134.00	23598.8	0.0042
26	134.18	23631.3	0.0092
27	134.40	23669.0	0.0037

HRMS Characterization

Figure S.8 – HRMS of *Azadipyrromethene* **3**

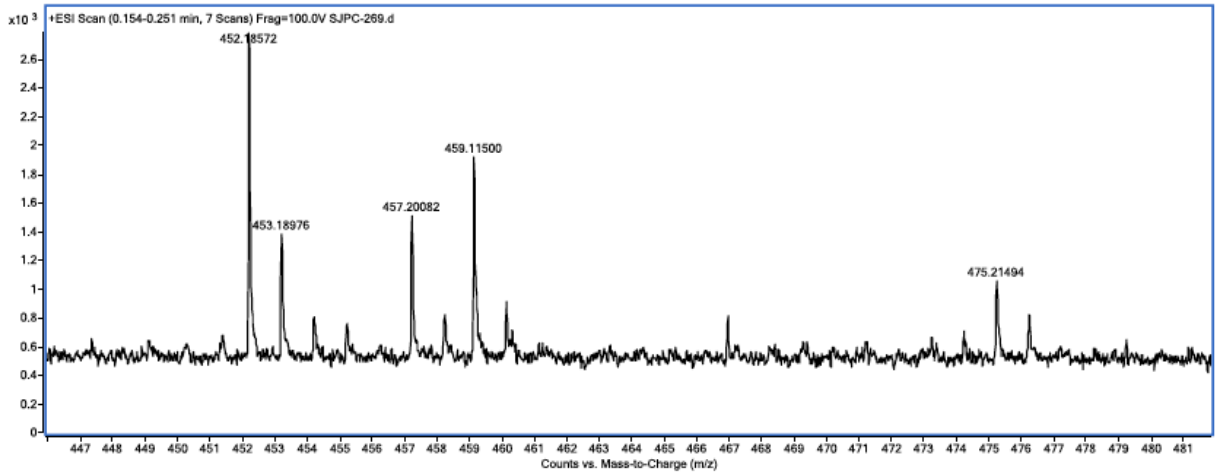

MS Spectrum Peak List

Ion	Ion Formula	Abund	*Expe. m/z*	*Calc. m/z*	Diff(ppm)
(M+H)+	C30H21N5		452.18572	452.18697	2.77

Figure S.9 – HRMS of *Azadipyrromethene* **4**

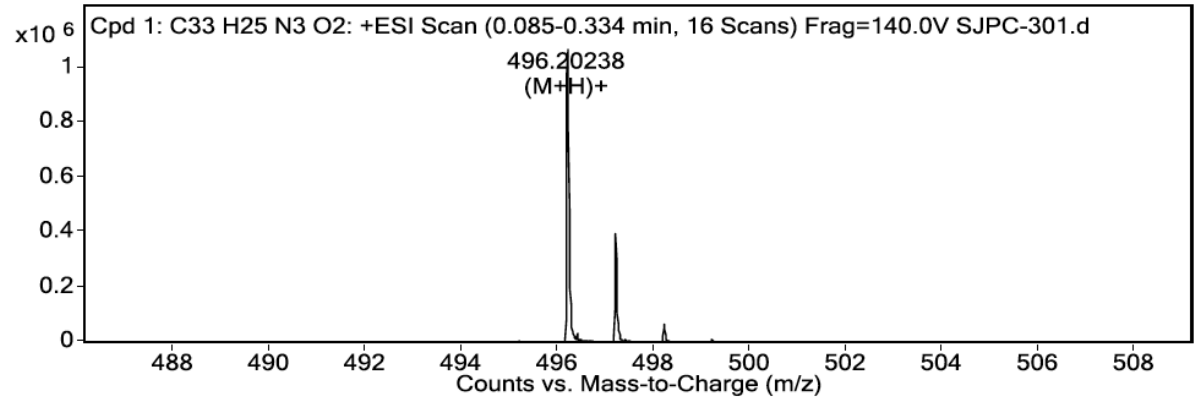

MS Spectrum Peak List

Ion	Formula	Abund	Observed m/z	Calc m/z	Diff (ppm)
(M+H)+	C33H25N3O2	1075282.31	496.20238	496.20195	-0.87

Figure S.10 – HRMS of *Azadipyrromethene* **5**

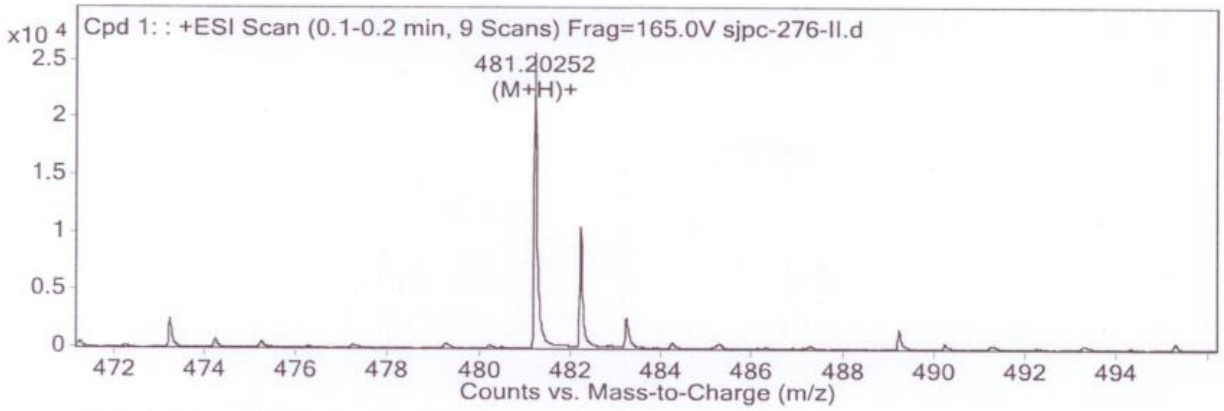

MS Spectrum Peak List

Ion	Ion Formula	Abund	*Expe. m/z*	*Calc. m/z*	Diff(ppm)
(M+H)+	C32H25N4O	25811.2	481.20252	481.20229	0.49

Figure S.11 – HRMS of *Azadipyrromethene* **6**

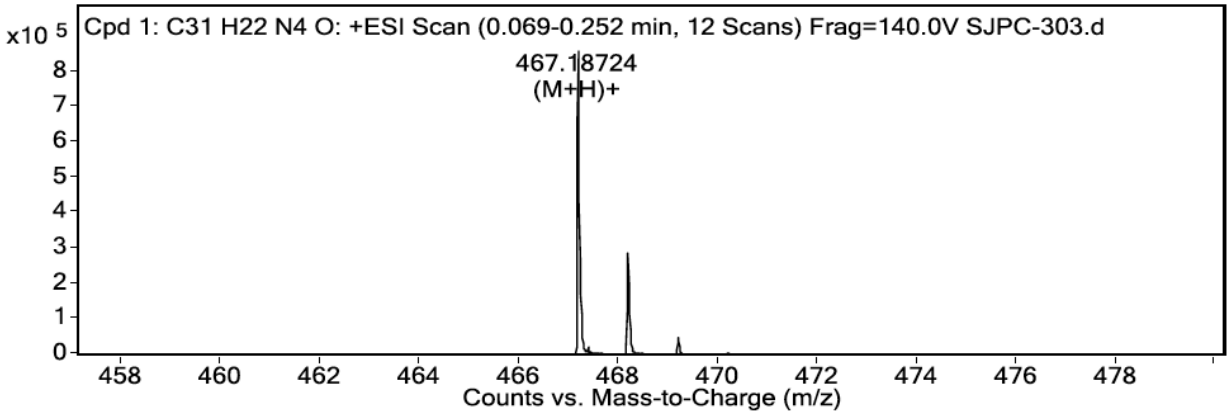

MS Spectrum Peak List

Ion	Formula	Abund	Observed m/z	Calc m/z	Diff (ppm)
(M+H)+	C31H22N4O	856545.24	467.18724	467.18664	-1.29

Electrochemistry

Figure S.12 – CV of ADPM **1** with ferrocene reference measured before and after due to interaction with the compound.
(0.46V vs SCE in DCM) (Scan rate of 50 mV/s at R.T.)

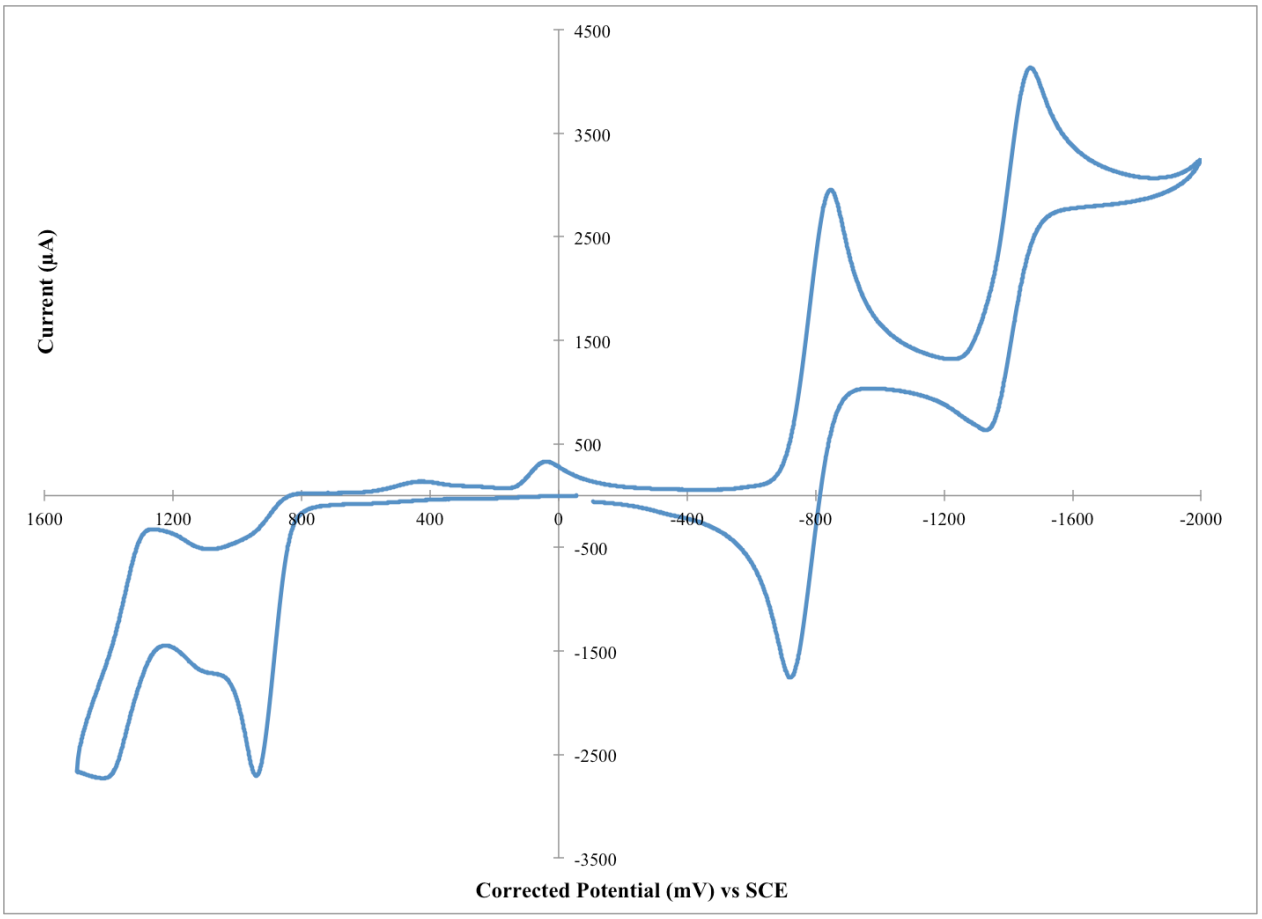

Figure S.13 – DPV of ADPM **1** with ferrocene reference measured before and after due to interaction with the compound.

(0.46V vs SCE in DCM) (Scan rate of 50 mV/s at R.T.)

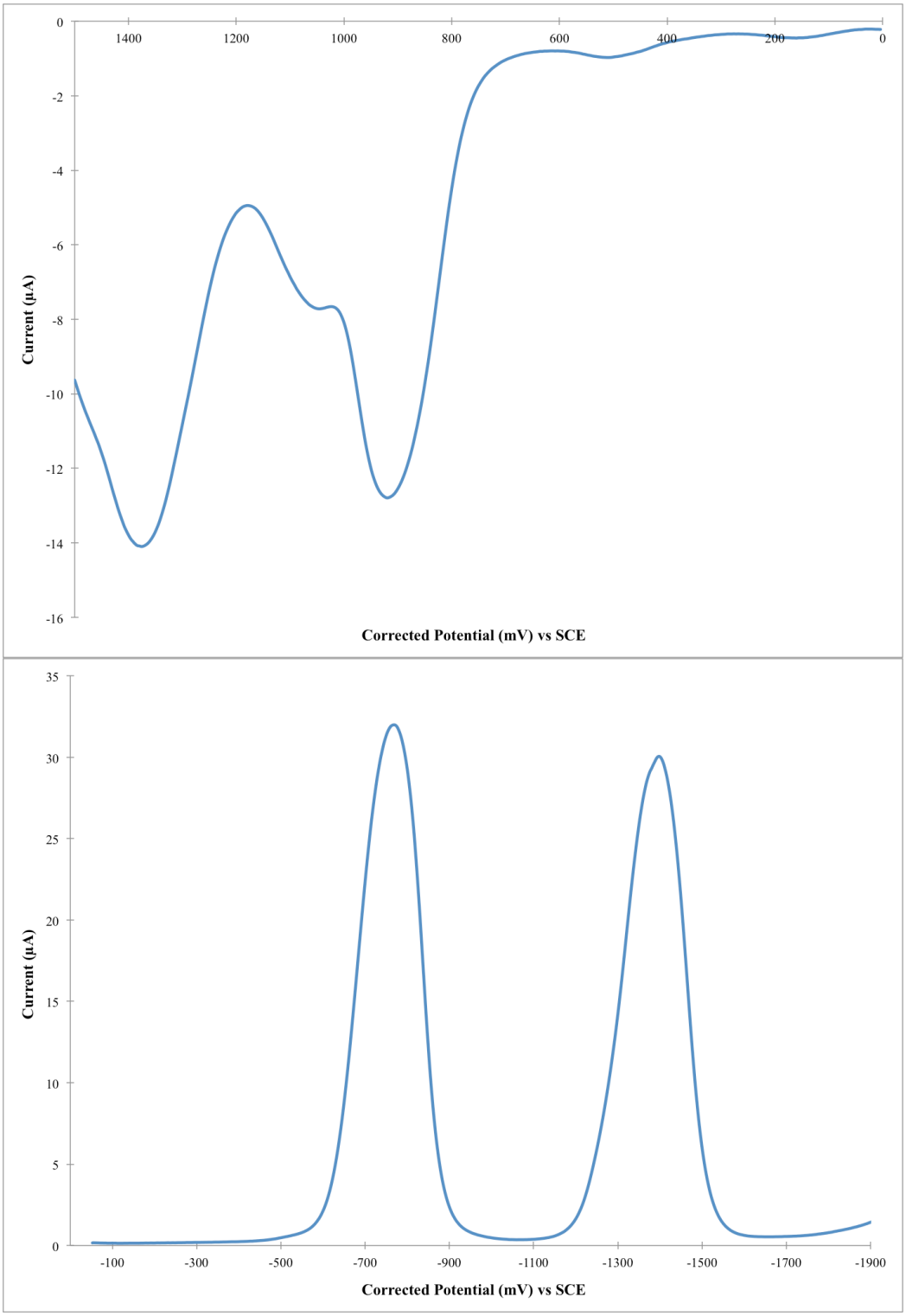

Figure S.14 – CV of ADPM **2** with ferrocene as internal reference.
(0.46V vs SCE in DCM) (Scan rate of 50 mV/s at R.T.)

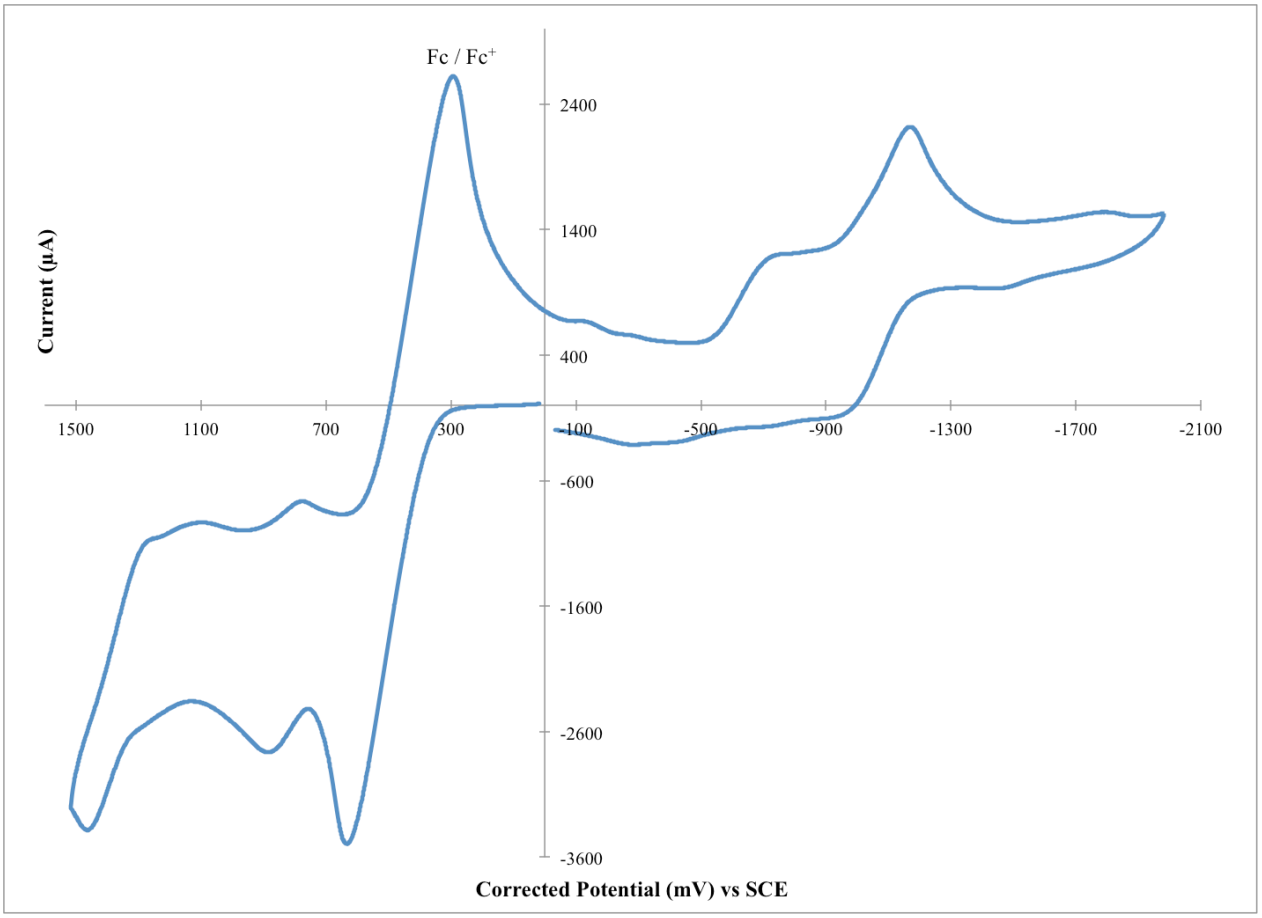

Figure S.15 – DPV of ADPM **2** with ferrocene as internal reference.
(0.46V vs SCE in DCM) (Scan rate of 50 mV/s at R.T.)

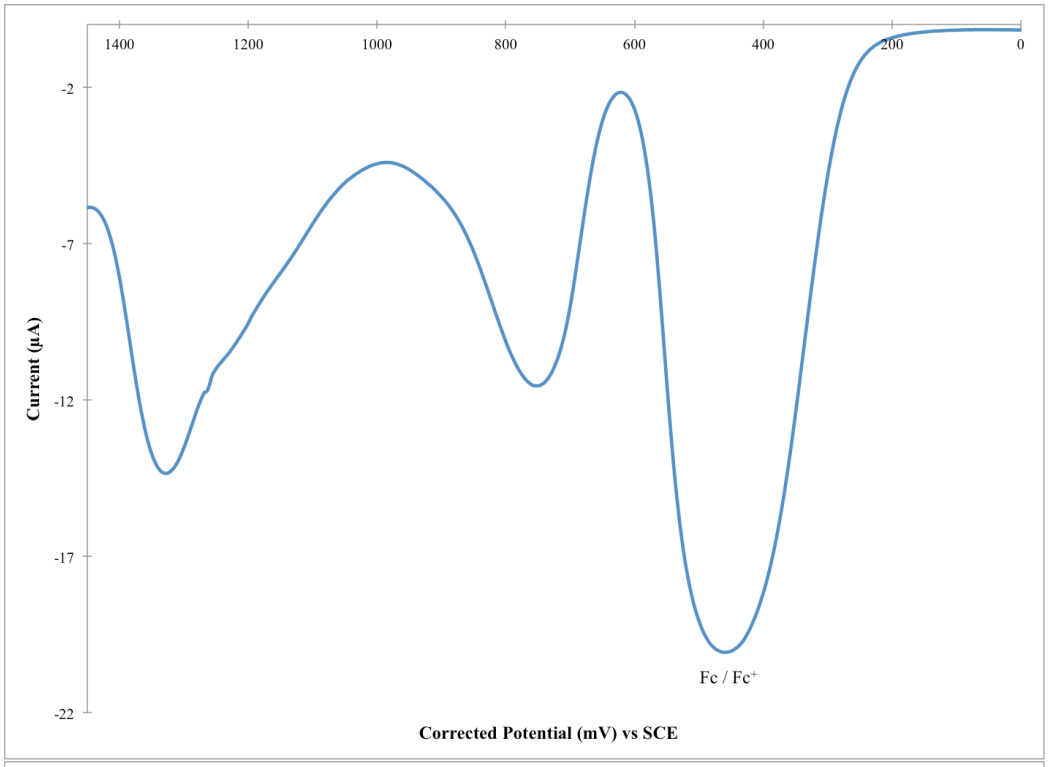

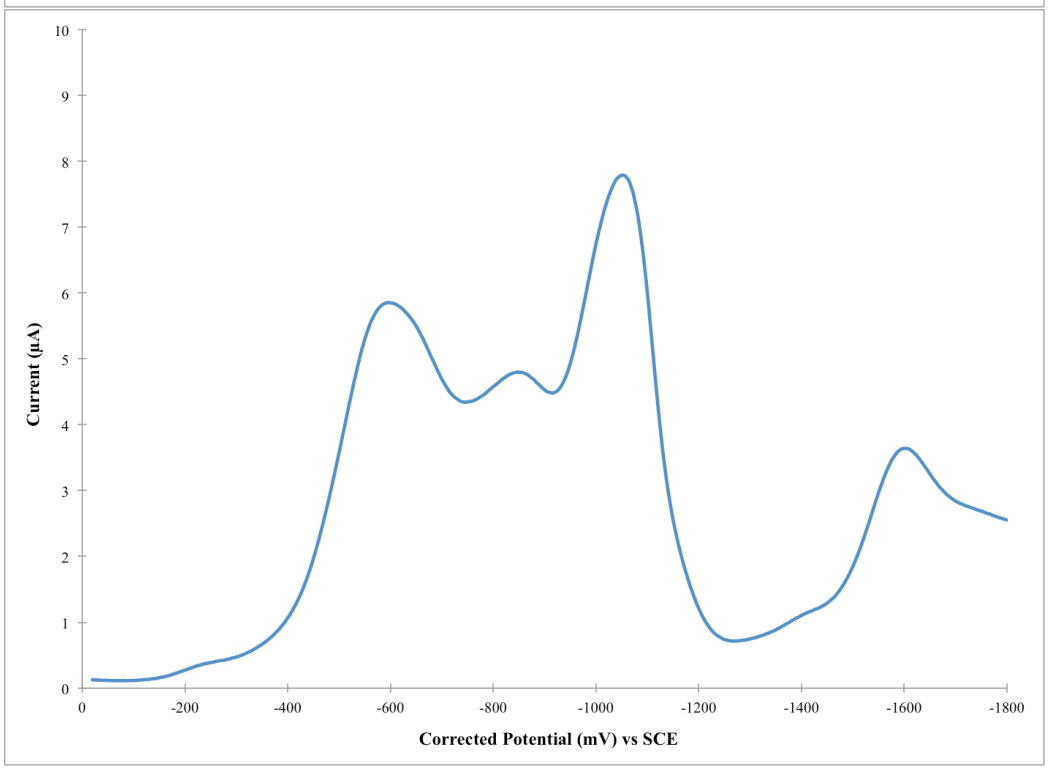

Figure S.16 – CV of ADPM **3** with ferrocene as internal reference.
(0.46V vs SCE in DCM) (Scan rate of 50 mV/s at R.T.)

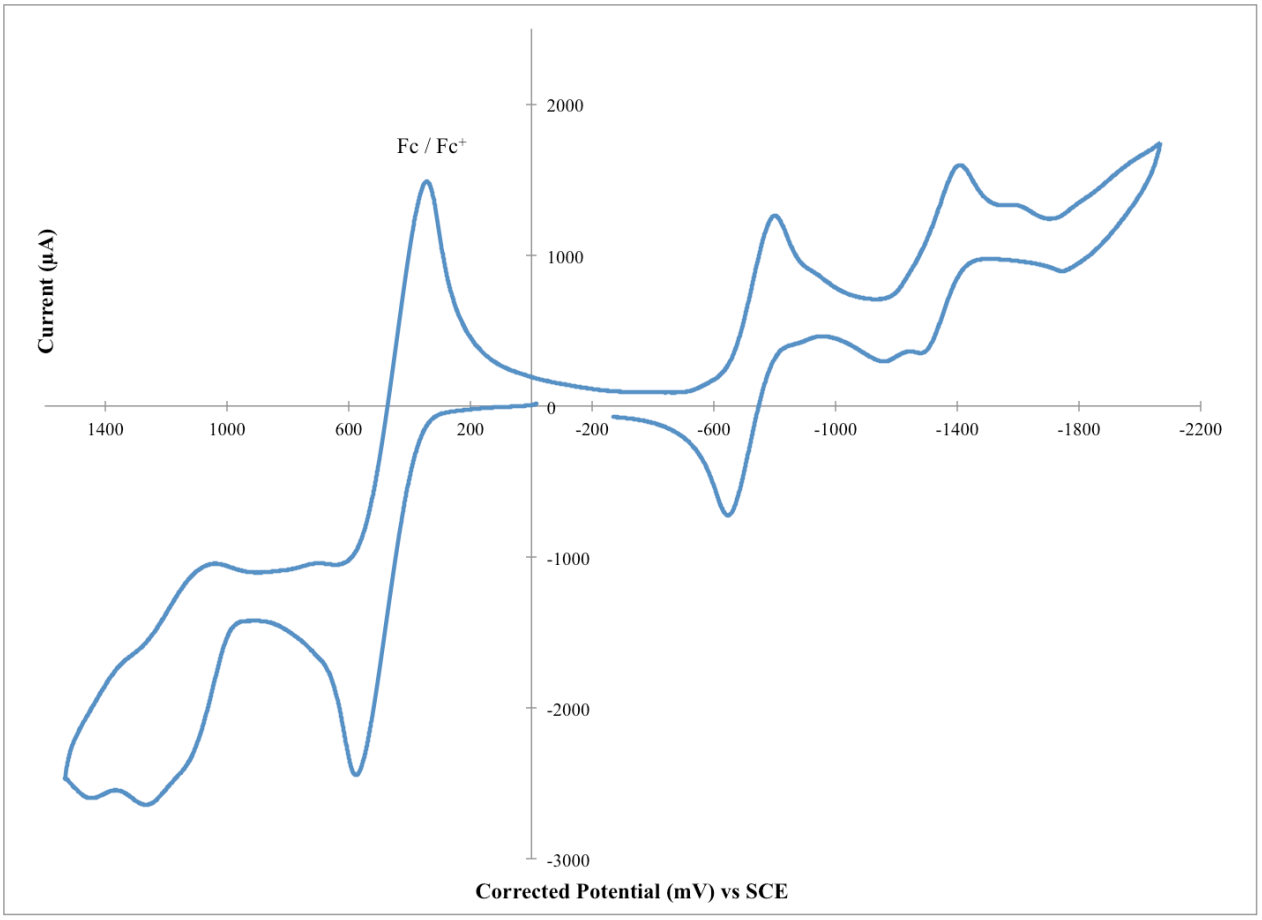

Figure S.17 – DPV of ADPM **3** with ferrocene as internal reference.
(0.46V vs SCE in DCM) (Scan rate of 50 mV/s at R.T.)

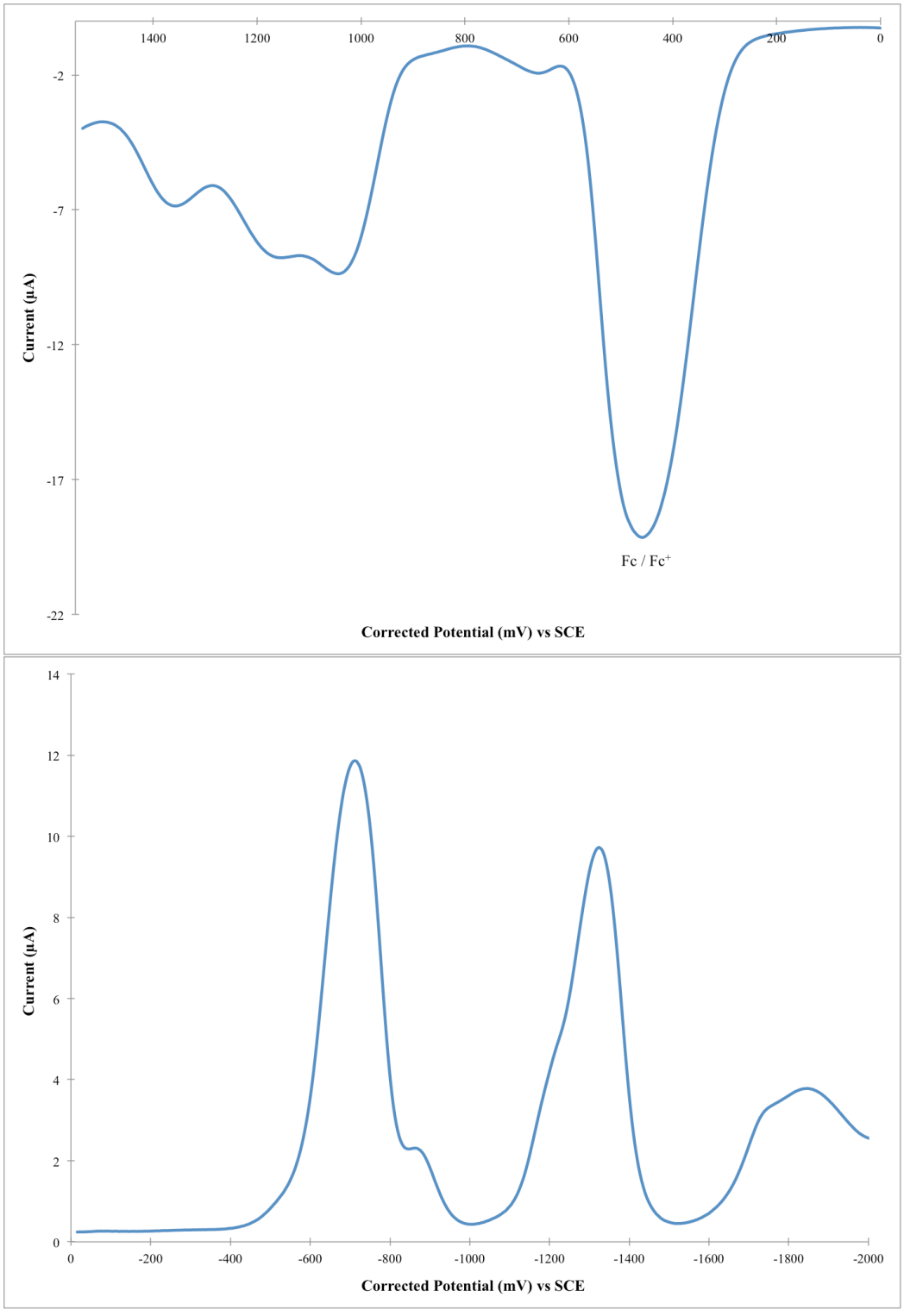

Figure S.18 – CV of ADPM **4** with ferrocene as internal reference.
(0.46V vs SCE in DCM) (Scan rate of 50 mV/s at R.T.)

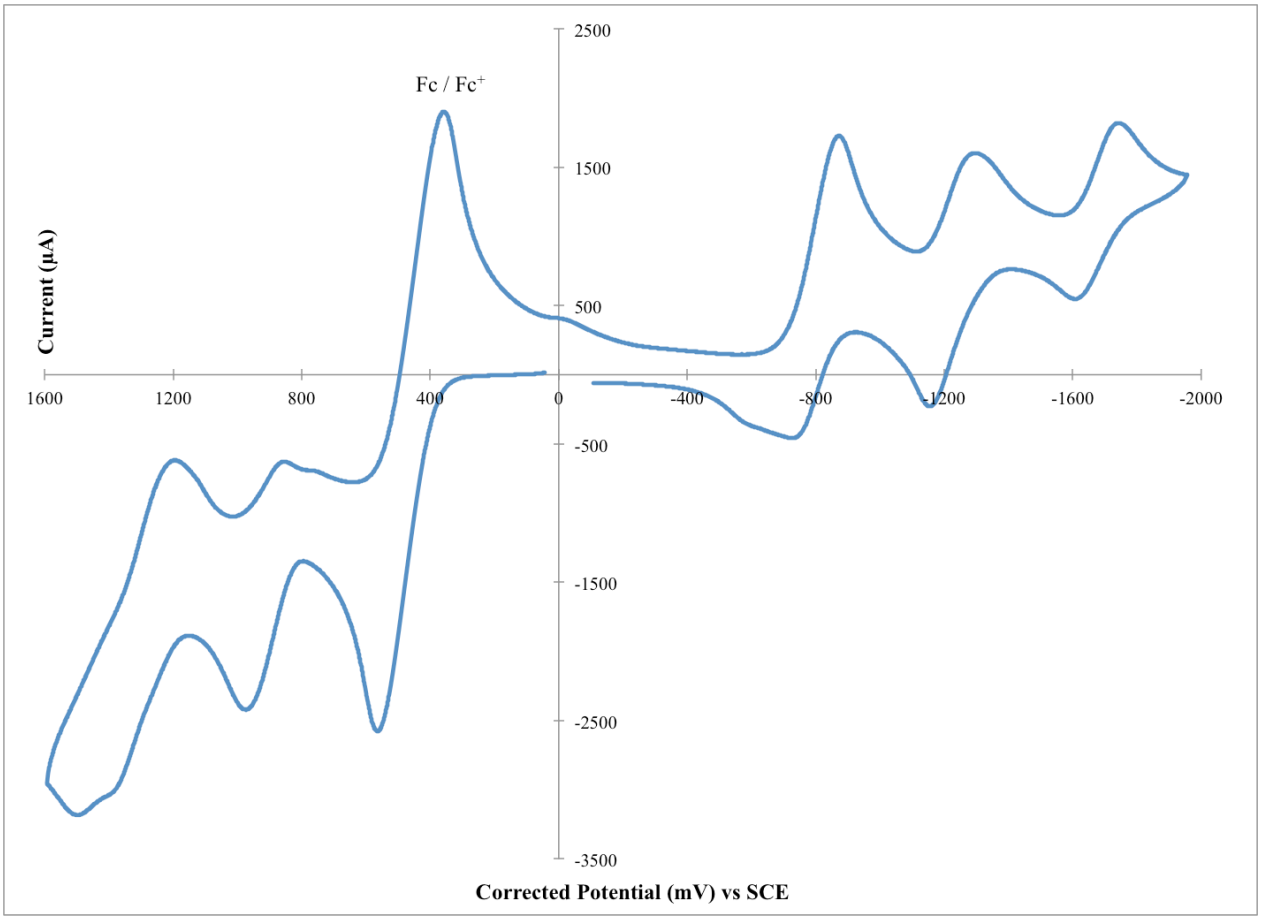

Figure S.19 – DPV of ADPM **4** with ferrocene as internal reference.
(0.46V vs SCE in DCM) (Scan rate of 50 mV/s at R.T.)

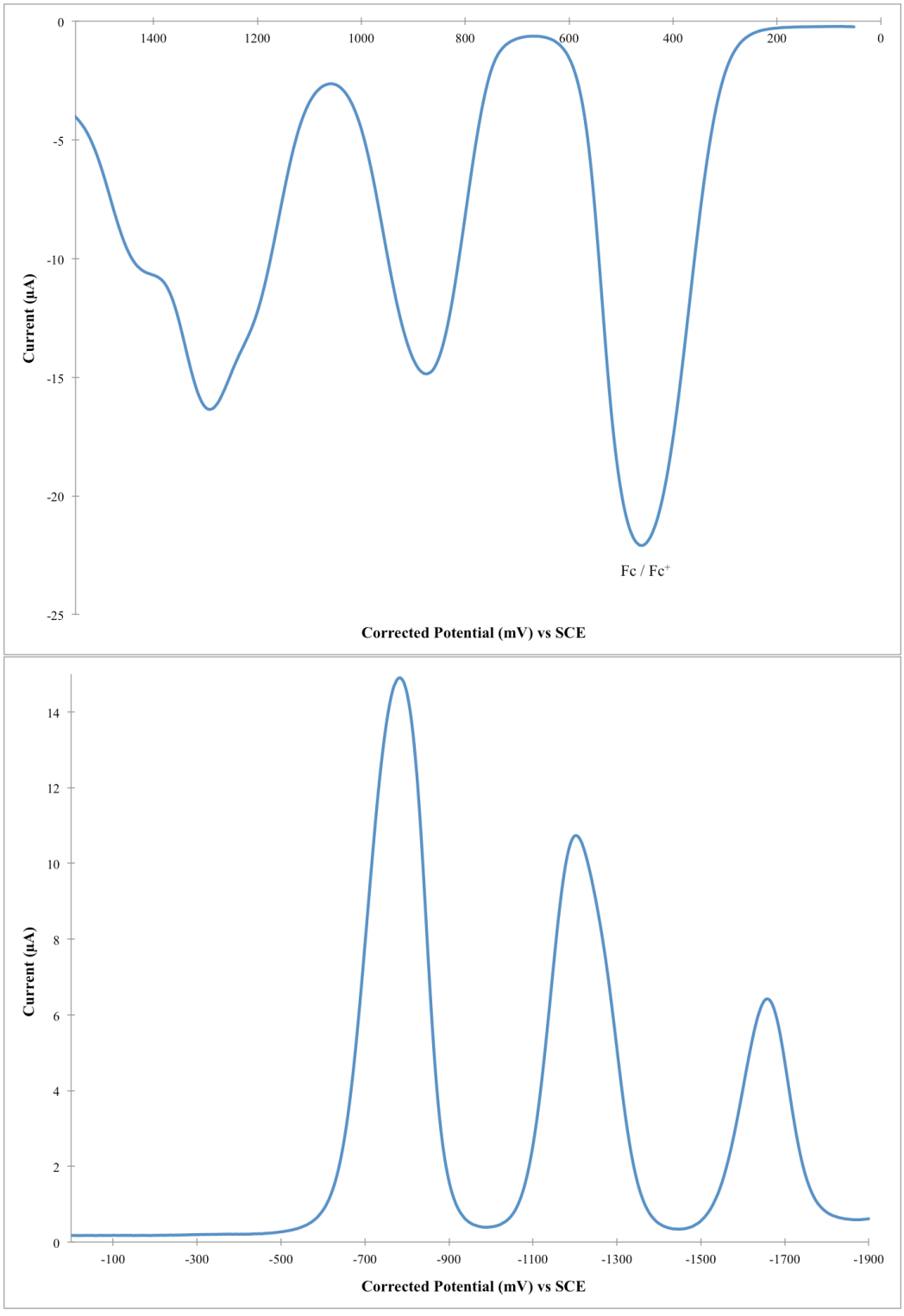

Figure S.20 – CV of ADPM **5** with ferrocene as internal reference.

(0.46V vs SCE in DCM) (Scan rate of 50 mV/s at R.T.)

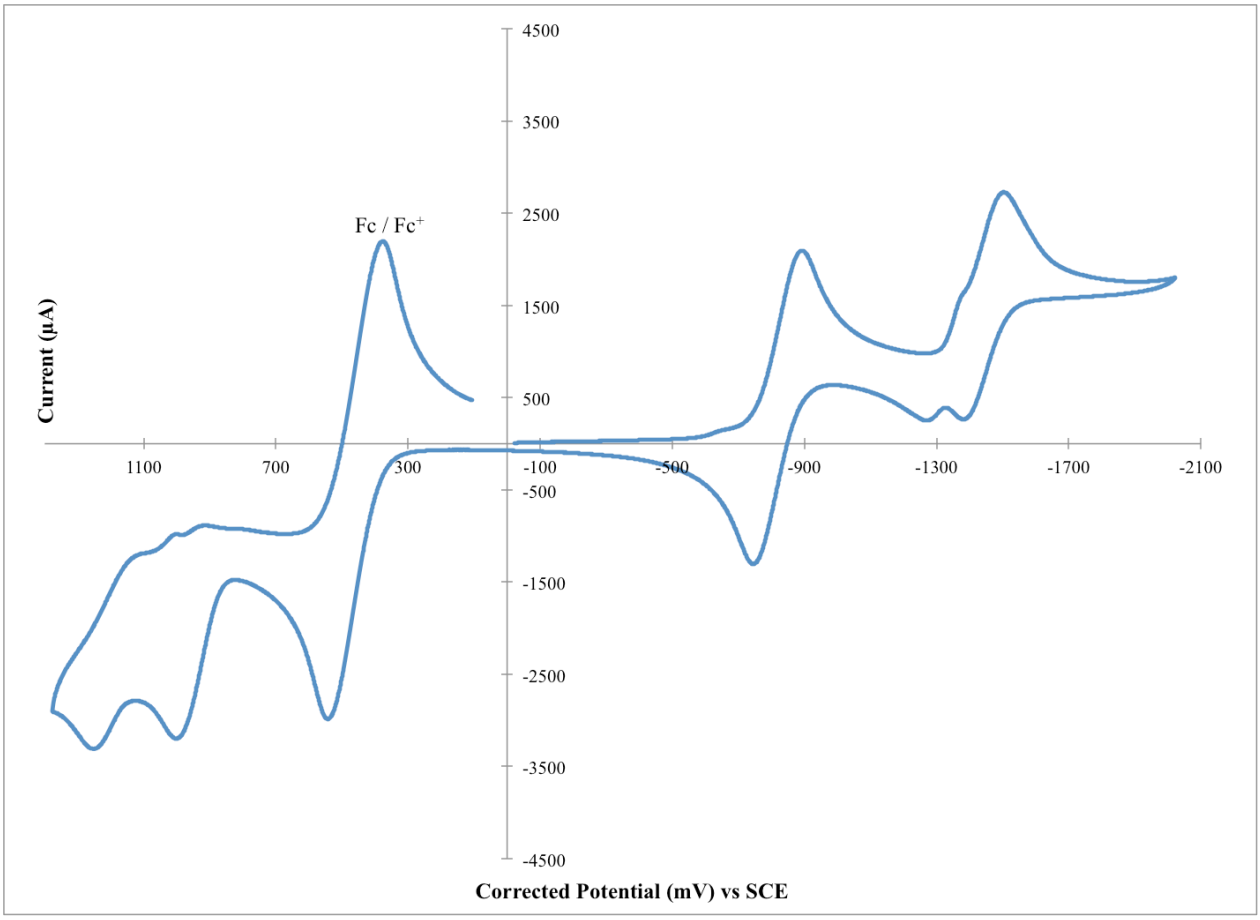

Figure S.21 – DPV of ADPM **5** with ferrocene as internal reference.
(0.46V vs SCE in DCM) (Scan rate of 50 mV/s at R.T.)

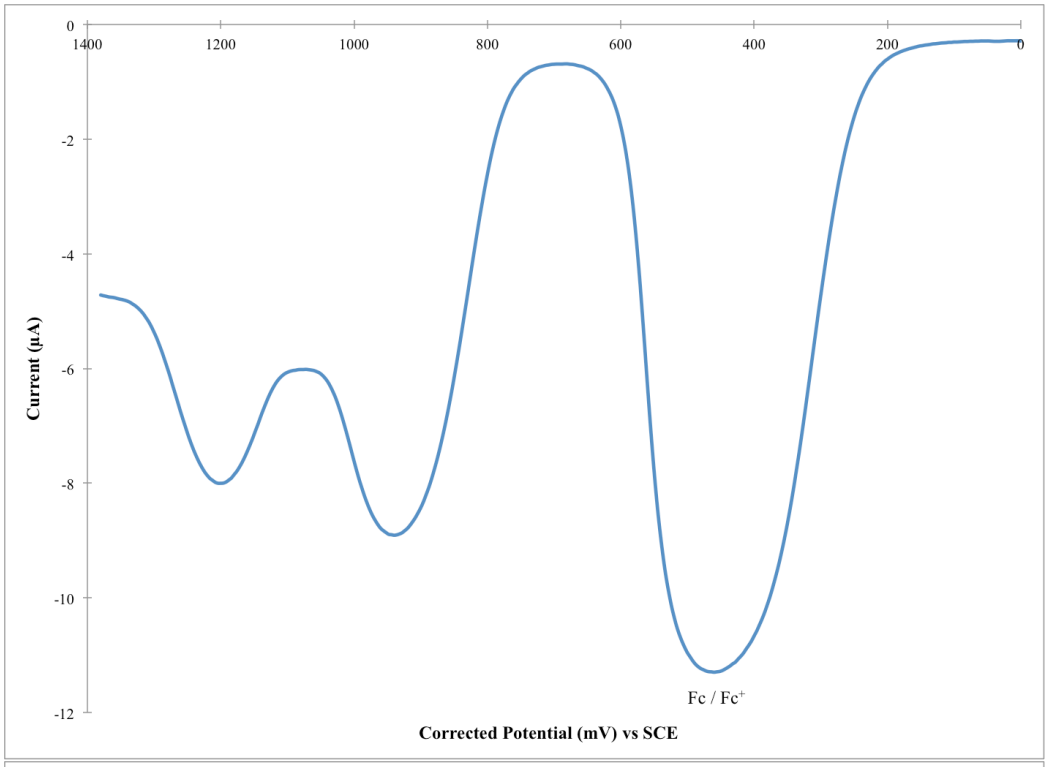

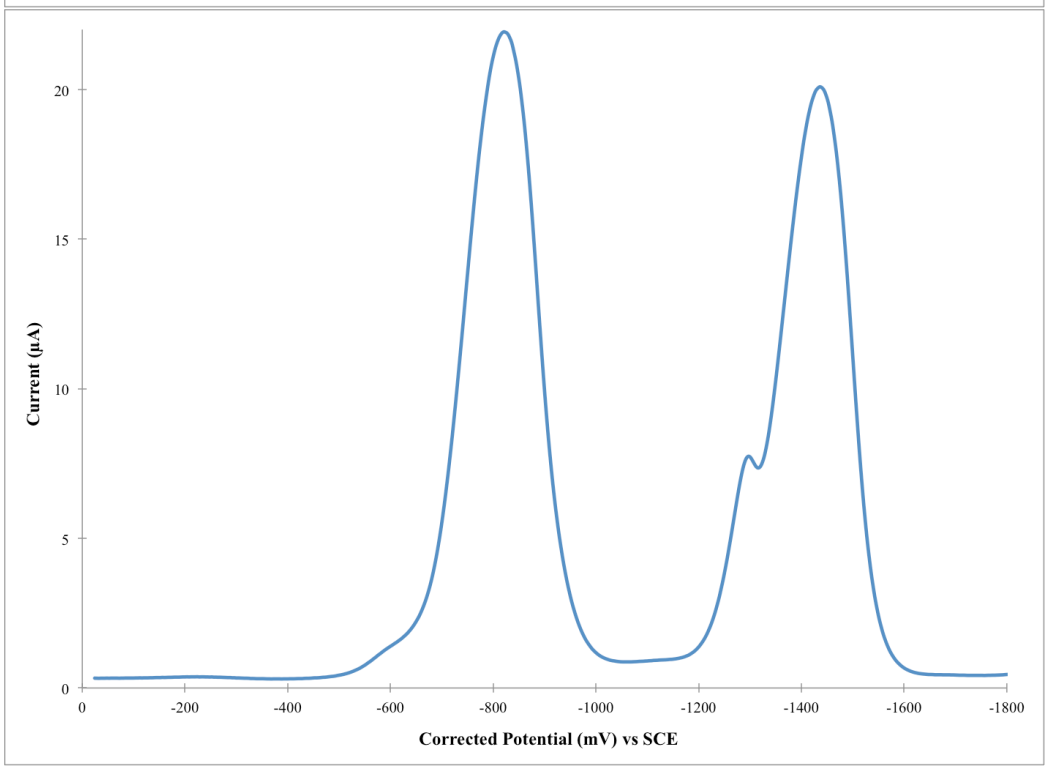

Figure S.22 – CV of ADPM **6** with ferrocene as internal reference.
(0.46V vs SCE in DCM) (Scan rate of 50 mV/s at R.T.)

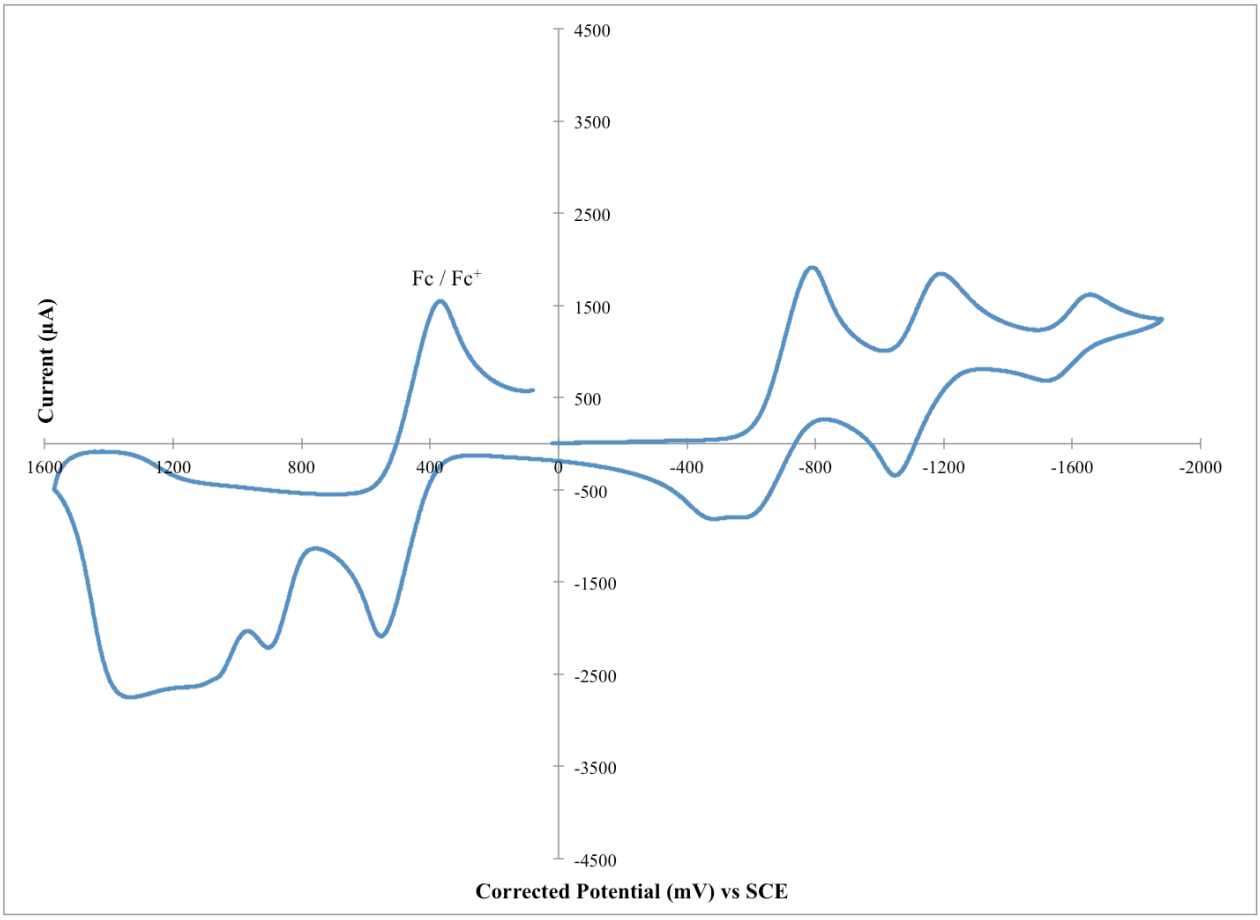

Figure S.23 – DPV of ADPM **6** with ferrocene as internal reference.
(0.46V vs SCE in DCM) (Scan rate of 50 mV/s at R.T.)

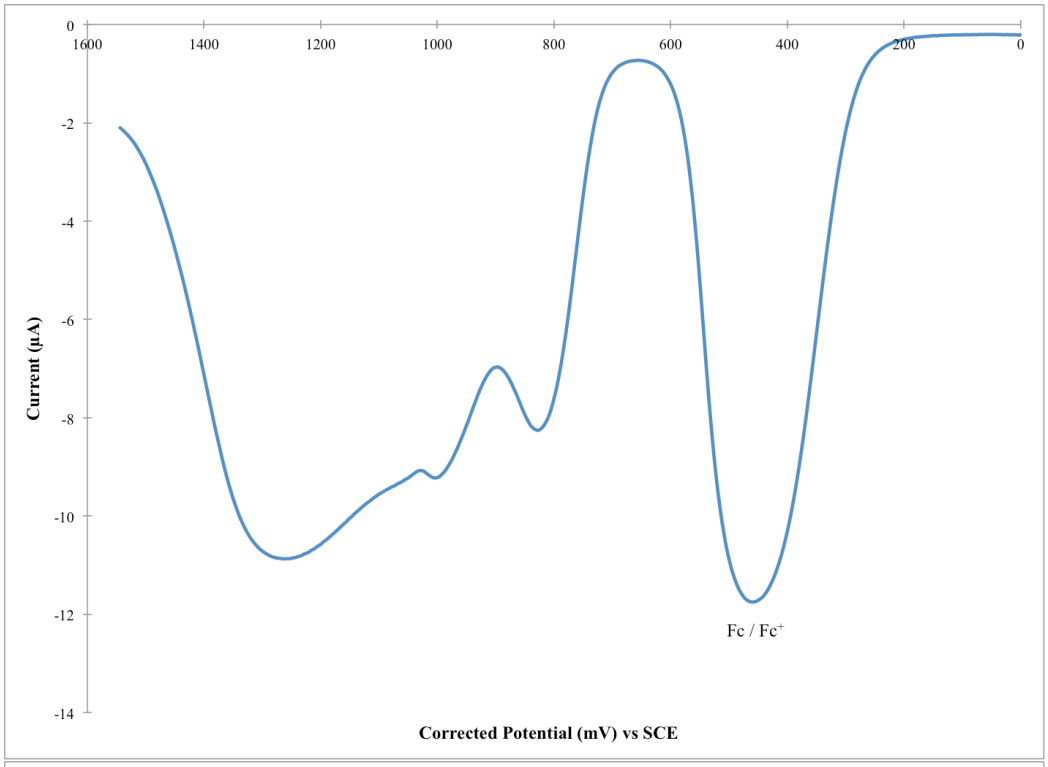

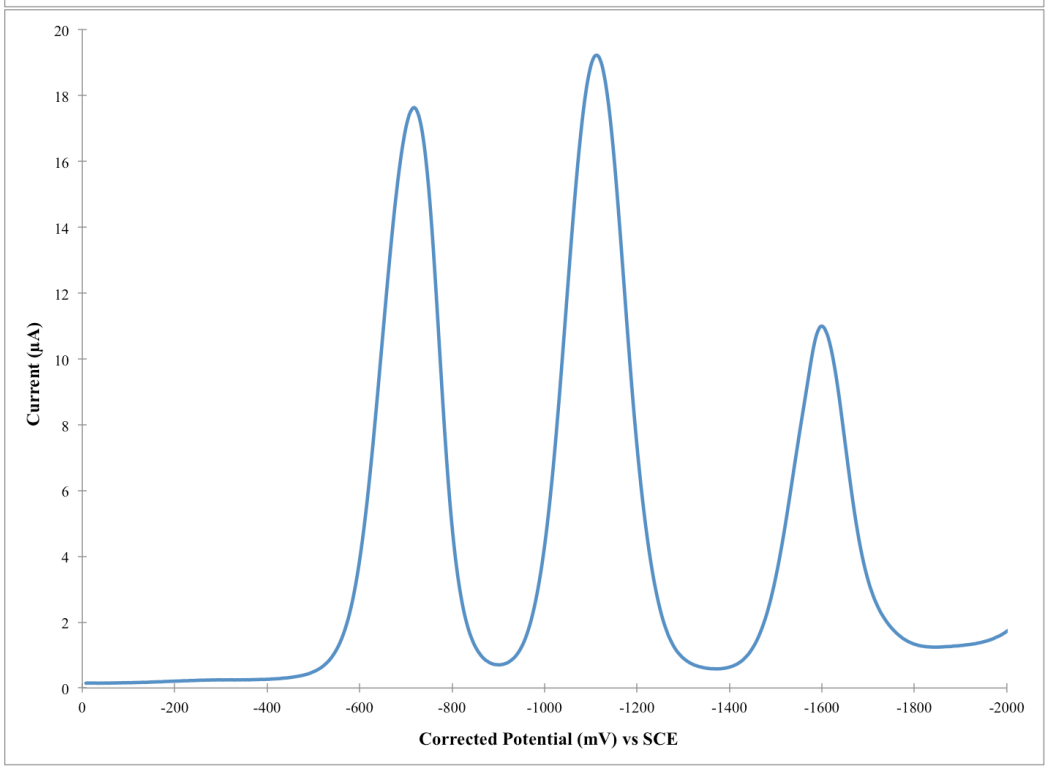

Computational Modelization

Figure S.24 – Representation of molecular orbital's energy levels (in eV) of ADPM derivatives **1** – **8** as obtained by DFT computational modelization and the corresponding band gap (occupied orbitals = blue; virtual orbitals = red).

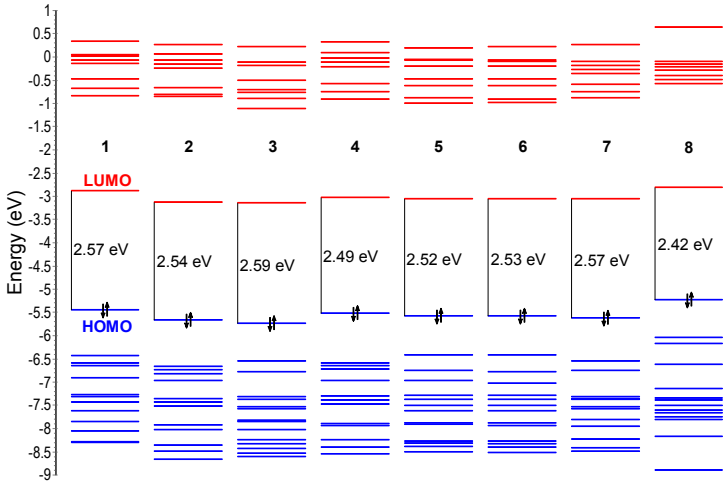

Table S.1 - Electronic distribution (%) on HOMO and LUMO for ADPM derivatives **1** – **8** as obtained by DFT computational modelization (r-pbe0 / 6-311g(2d,p); CPCM = CH_2Cl_2). [a), b)]

(Refer to Figure 5 for division of ADPM chromophore in computational modelization analysis)

	Molecular Orbital	**ADPM**	**Proximal Ar_1**	**Proximal Ar_2**	**Distal $Ar_{1'}$**	**Distal $Ar_{2'}$**
1	HOMO	62	17	11	6	4
	LUMO	66	8	14	6	5
2	HOMO	59	15	16	6	3
	LUMO	65	9	16	6	5
3	HOMO	68	12	8	8	4
	LUMO	70	7	11	7	5
4	HOMO	60	17	14	5	4
	LUMO	66	8	15	6	5
5	HOMO	66	18	7	5	4
	LUMO	67	8	11	4	10
6	HOMO	66	17	8	5	4
	LUMO	67	8	11	4	10
7	HOMO	66	13	9	7	4
	LUMO	63	12	14	6	5
8	HOMO	54	17	12	11	6
	LUMO	61	12	14	6	6

a) Ar1 is the aryl on the pyrrole side of the ADPM.

b) Distal Ar = Ph, otherwise stated. The prime number (#') in subscript corresponds to the distal aryl on the same side as the proximal one.

Table S.2 - Assignment of optical absorption bands of ADPM **1** in CH_2Cl_2 based on TD-DFT calculations (TD-BMK/6-311+G(2d,p); CPCM = CH_2Cl_2).

λ, nm		**Excitation**	**Assignation**
Observed (ε, x10^3 $M^{-1}cm^{-1}$)	**Calculated** (Osc. Strength)		
605 (47)	553 (0.834)	H -> L (99%)	Prox_1 -> ADPM
407 (6.8)	422 (0.040)	H-1 -> L (94%)	Dist_2 -> ADPM
	368 (0.252)	H-2 (77%), H-3 (16%) -> L	Periphery (except Dist_2) -> ADPM
	356 (0.168)	H-3 (79%), H-2 (16%) -> L	Prox_2 + Dist_1 -> ADPM
	349 (0.005)	H-8 (59%), H-9 (17%), H-6 (14%) -> L	Prox_1 + Dist_2 -> ADPM
299 (34)	320 (0.062)	H-4 -> L (92%)	Prox 1+2 -> Dist 1+2 + ADPM
	305 (0.004)	H-10 (38%), H-12 (32%), H-6 (12%), H-8 (10%) -> L	Dist 1+2 --> Prox 1+2 + ADPM
	297 (0.264)	H -> L+1 (80%)	ADPM + Side 2 --> Side 1
	296 (0.015)	H-5 -> L (78%)	Dist 1+2 --> Prox 1+2 + ADPM
	288 (0.433)	H-7 -> L (72%); H -> L+1 (10%)	Prox_2 --> ADPM

Figure S.25 – Experimental absorption spectrum in CH_2Cl_2 vs calculated optical absorption bands of ADPM **1** based on TD-DFT calculations (TD-BMK/6-311+G(2d,p); CPCM = CH_2Cl_2).

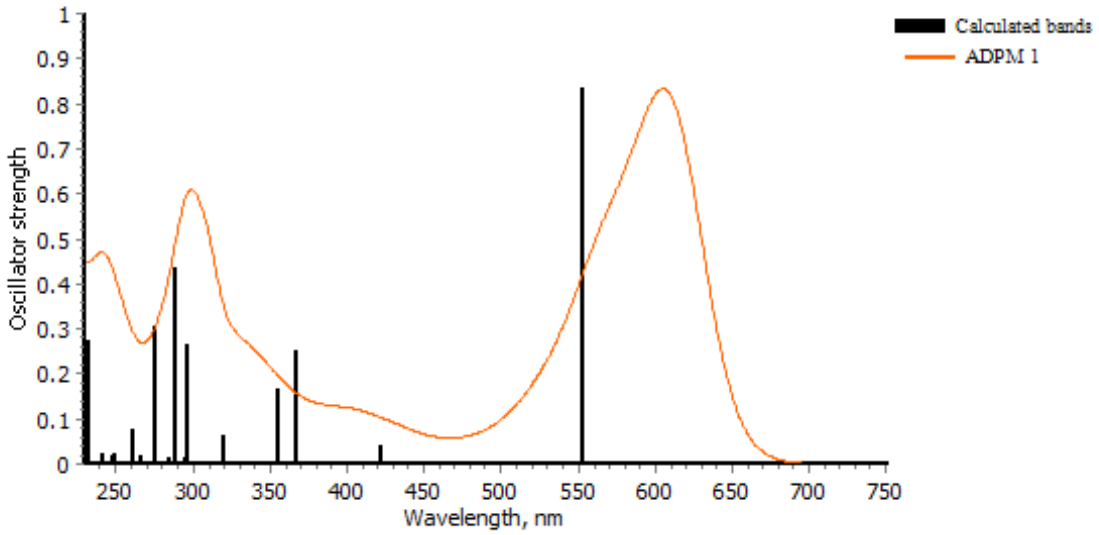

Table S.3 - Assignment of optical absorption bands of ADPM **2** in CH_2Cl_2 based on TD-DFT calculations (TD-BMK/6-311+G(2d,p); CPCM = CH_2Cl_2).

λ, nm		**Excitation**	**Assignation**
Observed (ε, x10^3 $M^{-1}cm^{-1}$)	**Calculated** (Osc. Strength)		
615 (39) and 577	560 (0.834)	H -> L (99%)	Side 1 -> ADPM
415 (6.0)	413 (0.093)	H-2 (70%), H-1 (22%) -> L	Periphery (except Dist_1) -> ADPM
	378 (0.130)	H-1 (73%), H-2 (17%) -> L	Periphery (except Dist_1) -> ADPM
	368 (0.233)	H-3 -> L (85%)	Side 1 -> ADPM
307 (26)	339 (0.008)	H-9 (53%), H-4 (20%), H-6 (14%) -> L	Periphery (except Prox_2) -> ADPM
	332 (0.092)	H-4 (70%), H-9 (15%) -> L	Prox_1 -> ADPM
	309 (0.003)	H-5 -> L (86%)	Dist 1+2 + Prox_1 -> ADPM + Prox_2
	303 (0.026)	H-7 (58%), H-6 (17%) -> L	Periphery -> ADPM
	297 (0.026)	H-6 (48%), H-7 (24%), H-9 (13%), H-5 (11%) -> L	Periphery -> ADPM
	283 (0.023)	H-12 (34%), H-10 (28%), H-8 (12%) -> L; H -> L+1 (10%)	Periphery -> ADPM

Figure S.26 – Experimental absorption spectrum in CH_2Cl_2 vs calculated optical absorption bands of ADPM **2** based on TD-DFT calculations (TD-BMK/6-311+G(2d,p); CPCM = CH_2Cl_2).

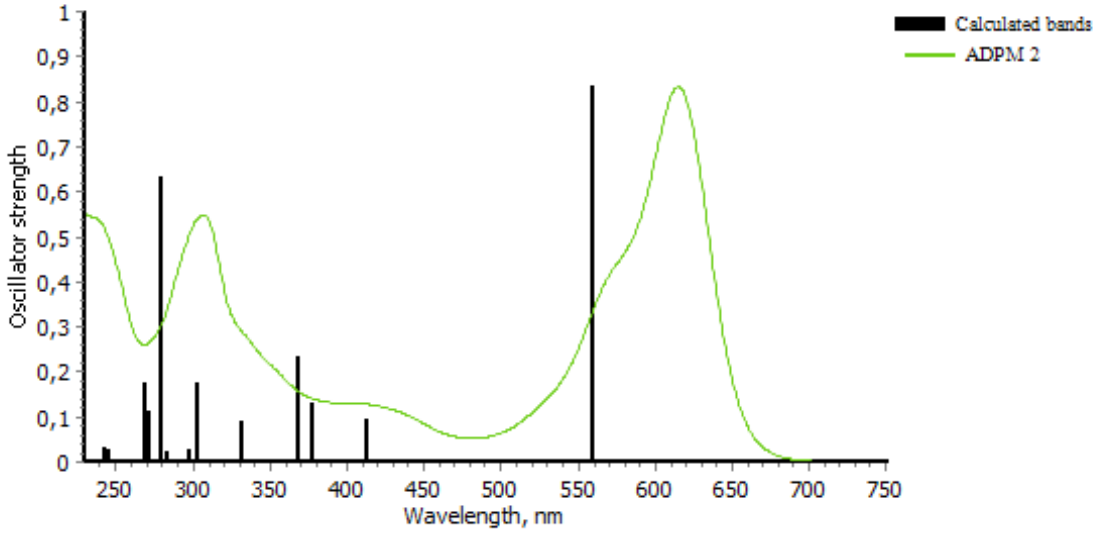

Table S.4 - Assignment of optical absorption bands of ADPM **3** in CH_2Cl_2 based on TD-DFT calculations (TD-BMK/6-311+G(2d,p); CPCM = CH_2Cl_2).

λ, nm		**Excitation**	**Assignation**
Observed (ε, x10^3 $M^{-1}cm^{-1}$)	**Calculated** (Osc. Strength)		
590 (39) and 558	547 (0.877)	H -> L (99%)	Side 1 -> Side 2 + ADPM
--	441 (0.064)	H-1 -> L (95%)	Dist_2 -> Periphery + ADPM
--	381 (0.164)	H-2 -> L (94%)	Dist_1 -> Periphery + ADPM
307 (30)	357 (0.006)	H-9 (37%), H-7 (20%), H-6 (18%), H-4 (12%) -> L	Periphery -> ADPM
	328 (0.003)	H-6 -> L (56%)	Periphery (except Dist_1) -> ADPM
	311 (0.000)	H-3 -> L (86%)	Dist 1+2 -> ADPM + Prox 1+2
	305 (0.076)	H-5 (35%), H-4 (20%), H-7 (13%) -> L	Periphery -> ADPM
	299 (0.026)	H-4 (34%), H-5 (33%), H-9 (10%) -> L; H -> L+1 (11%)	Periphery (except Prox_1) -> Prox_1 + ADPM
	293 (0.266)	H -> L+1 (37%); H-14 (15%), H-4 (10%) -> L	Periphery (except Prox_1) -> Prox_1 + ADPM
	289 (0.826)	H -> L+1 (37%); H-5 (21%), H-14 (15%) -> L	Periphery (except Prox_1) -> Prox_1 + ADPM

Figure S.27 – Experimental absorption spectrum in CH_2Cl_2 vs calculated optical absorption bands of ADPM **3** based on TD-DFT calculations (TD-BMK/6-311+G(2d,p); CPCM = CH_2Cl_2).

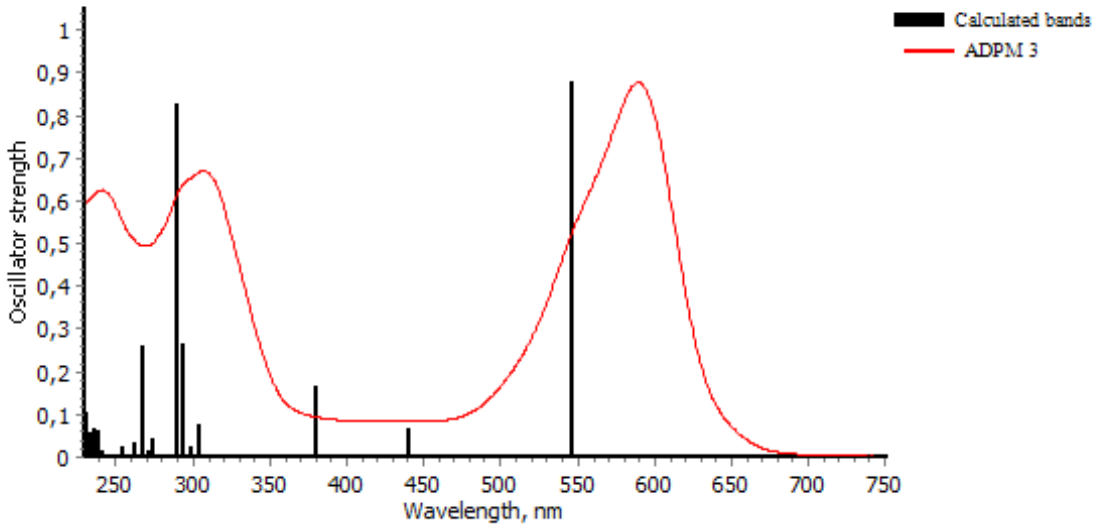

Table S.5 - Assignment of optical absorption bands of ADPM **4** in CH_2Cl_2 based on TD-DFT calculations (TD-BMK/6-311+G(2d,p); CPCM = CH_2Cl_2).

λ, nm		**Excitation**	**Assignation**
Observed (ε, x10^3 $M^{-1}cm^{-1}$)	**Calculated** (Osc. Strength)		
602 (33) and 567 (24)	571 (0.861)	H -> L (99%)	Prox_1 + Prox_2 + Dist_1 -> Dist_2 + ADPM
417 (8.3)	409 (0.070)	H-2 -> L (87%)	Dist 1+2 -> Prox_2 + ADPM
	374 (0.380)	H-1 -> L (88%)	Periphery -> ADPM
	370 (0.019)	H-3 -> L (86%)	Prox_2 + Dist 1+2 -> Prox_1 + ADPM
298 (30)	340 (0.009)	H-9 (64%), H-6 (15%) -> L	Dist 1+2 -> Prox_2 + ADPM
	328 (0.089)	H-4 -> L (84%)	Prox_1 -> Dist_2 + ADPM
	304 (0.002)	H-5 -> L (89%)	Dist 1+2 -> Prox 1+2 +
	301 (0.024)	H-7 (50%), H-6 (12%) -> L; H -> L+1 (23%)	Prox_2 + Dist 1+2 -> Prox_1 + ADPM
	294 (0.374)	H -> L+1 (48%); H-6 (29%), H-9 (10%) -> L	Prox_2 + Dist 1+2 -> Prox_1 + ADPM
	292 (0.347)	H-7 (32%), H-6 (27%) -> L; H -> L+1 (22%)	Prox_2 + Dist 1+2 -> Prox_1 + ADPM

Figure S.28 – Experimental absorption spectrum in CH_2Cl_2 vs calculated optical absorption bands of ADPM **4** based on TD-DFT calculations (TD-BMK/6-311+G(2d,p); CPCM = CH_2Cl_2).

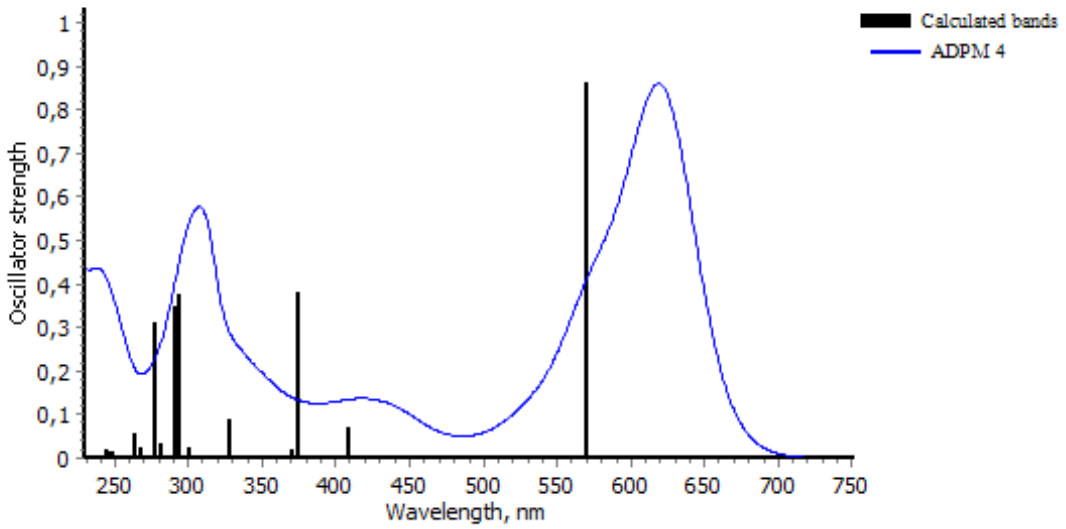

Table S.6 - Assignment of optical absorption bands of ADPM **5** in CH_2Cl_2 based on TD-DFT calculations (TD-BMK/6-311+G(2d,p); CPCM = CH_2Cl_2).

λ, nm		**Excitation**	**Assignation**
Observed (ε, x10^3 $M^{-1}cm^{-1}$)	**Calculated** (Osc. Strength)		
619 (52) and 576 (28)	566 (0.830)	H -> L (99%)	Prox_1 -> Prox_2 + Dist_2 + ADPM
417 (3.9)	445 (0.051)	H-1 -> L (96%)	Dist_2 -> Periphery + ADPM
	373 (0.228)	H-2 -> L (89%)	Side 1 -> Side 2 + ADPM
307 (35)	348 (0.021)	H-9 (43%), H-7 (32%) -> L	Prox_2 + Dist 1+2 -> Prox_1 + ADPM
	332 (0.085)	H-3 -> L (87%)	Side 1 -> Side 2 + ADPM
	308 (0.030)	H-7 (26%), H-13 (20%), H-4 (19%), H-5 (11%), H-6 (10%) -> L	Prox_2 + Dist 1+2 -> Prox_1 + ADPM
	306 (0.009)	H-4 -> L (74%)	Dist 1+2 -> Periphery + ADPM
	298 (0.060)	H-6 -> L (58%); H -> L+2 (17%)	Periphery (except Prox_1) -> ADPM
	294 (0.004)	H-5 (57%), H-9 (26%) -> L	Dist_1 + Prox_2 -> Prox_1 + Dist_2 + ADPM
	289 (0.749)	H -> L+1 (41%); H -> L+2 (35%)	ADPM -> Periphery (except Dist_1)

Figure S.29 – Experimental absorption spectrum in CH_2Cl_2 vs calculated optical absorption bands of ADPM **5** based on TD-DFT calculations (TD-BMK/6-311+G(2d,p); CPCM = CH_2Cl_2).

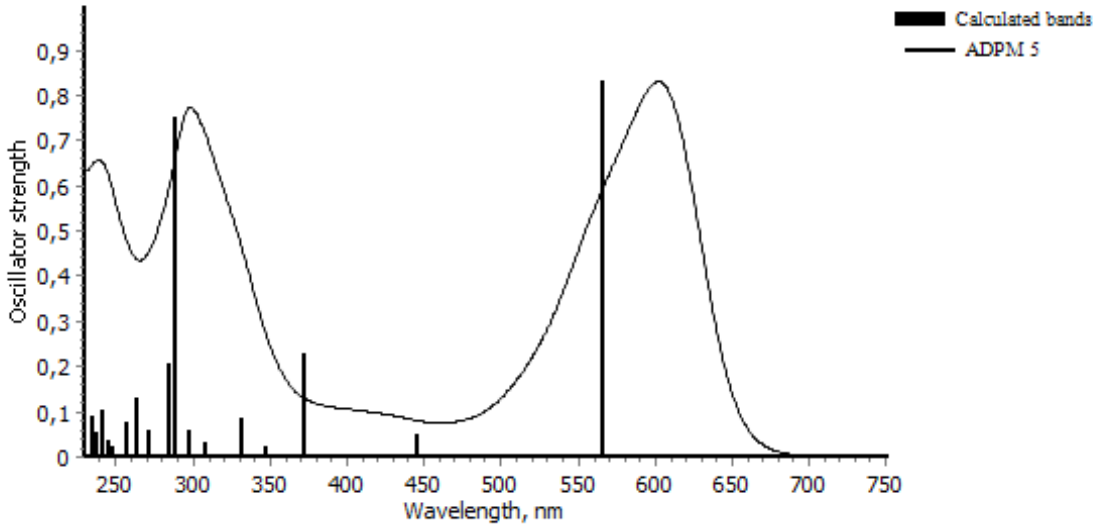

Table S.7 - Assignment of optical absorption bands of ADPM **6** in CH_2Cl_2 based on TD-DFT calculations (TD-BMK/6-311+G(2d,p); CPCM = CH_2Cl_2).

λ, nm		**Excitation**	**Assignation**
Observed (ε, x10^3 $M^{-1}cm^{-1}$)	**Calculated** (Osc. Strength)		
598 (43) and 561	564 (0.850)	H -> L (99%)	Prox_1 -> Side 2 + ADPM
418 (6.9)	446 (0.054)	H-1 -> L (96%)	Dist_2 -> Periphery + ADPM
	371 (0.203)	H-2 -> L (91%)	Side 1 -> Side 2 + ADPM
308 (36)	348 (0.018)	H-9 (45%), H-7 (33%) -> L	Prox_2 + Dist 1+2 -> Prox_1 + ADPM
	325 (0.091)	H-3 -> L (92%)	Prox_1 -> Side 2 + ADPM
	309 (0.034)	H-7 (26%), H-13 (20%), H-4 (15%), H-6 (12%), H-5 (11%) -> L	Prox_2 + Dist 1+2 -> Prox_1 + ADPM
	306 (0.009)	H-4->L (78%)	Dist 1+2 -> Prox 1+2 + ADPM
	299 (0.042)	H-6 -> L (55%); H -> L+2 (20%)	Prox_2 + Dist 1+2 -> Prox_1 + ADPM
	294 (0.003)	H-5 (57%), H-9 (26%) ->L	Dist_1 + Prox_2 -> Prox_1 + Dist_2 + ADPM
	290 (0.736)	H-6 -> L (10%); H -> L+1 (16%); H -> L+2 (53%)	ADPM -> Periphery (exept Prox_2)

Figure S.30 – Experimental absorption spectrum in CH_2Cl_2 vs calculated optical absorption bands of ADPM **6** based on TD-DFT calculations (TD-BMK/6-311+G(2d,p); CPCM = CH_2Cl_2).

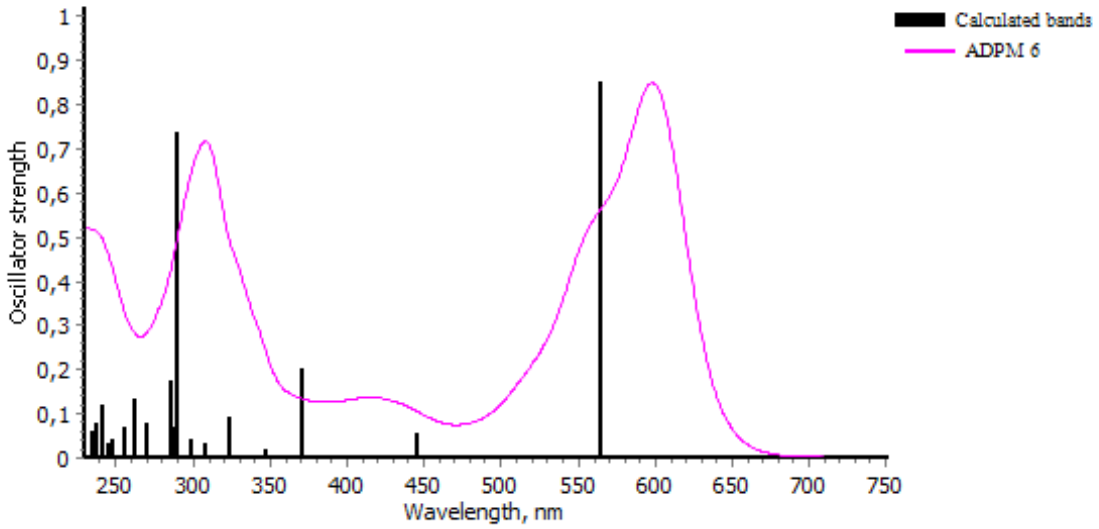

Table S.8 - Assignment of optical absorption bands of ADPM **7** in CH_2Cl_2 based on TD-DFT calculations (TD-BMK/6-311+G(2d,p); CPCM = CH_2Cl_2).

λ, nm		**Excitation**	**Assignation**
Observed (ε, x10^3 $M^{-1}cm^{-1}$)	**Calculated** (Osc. Strength)		
590 (40)	551 (0.885)	H -> L (99%)	Side 1 -> Side 2 + ADPM
--	428 (0.059)	H-1 -> L (96%)	Dist_2 -> Periphery + ADPM
--	372 (0.190)	H-2 -> L (97%)	Dist_1 -> Side 2 + ADPM
297 (43)	346 (0.003)	H-9 (61%), H-5 (16%), H-8 (13%) -> L	Prox_1 + Dist 1+2 -> Prox_2 + ADPM
	311 (0.261)	H-4 -> L (66%)	Periphery -> ADPM
	305 (0.000)	H-3 -> L (80%)	Dist 1+2 -> Prox 1+2 + ADPM
	299 (0.084)	H-5 (24%), H-12 (21%), H-4 (19%), H-10 (10%) -> L	Prox_2 + Dist 1+2 -> Prox_1 + ADPM
	293 (0.023)	H-6 (68%), H-5 (16%) ->L	Prox_2 + Dist 1+2 -> Prox_1 + ADPM
	291 (0.017)	H-5 (27%), H-10 (21%), H-12 (20%), H-6 (13%) -> L	Prox_2 + Dist 1+2 -> Prox_1 + ADPM
	286 (0.714)	H -> L+1 (79%)	ADPM + Side 2 -> Side 1

Figure S.31 – Experimental absorption spectrum in CH_2Cl_2 vs calculated optical absorption bands of ADPM **7** based on TD-DFT calculations (TD-BMK/6-311+G(2d,p); CPCM = CH_2Cl_2).

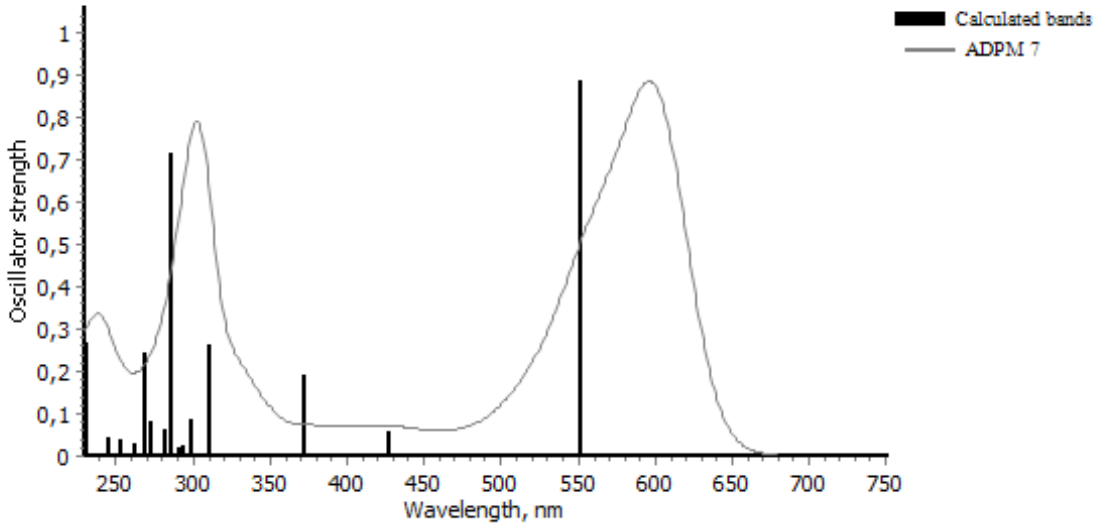

Table S.9 - Assignment of optical absorption bands of ADPM **8** in CH_2Cl_2 based on TD-DFT calculations (TD-BMK/6-311+G(2d,p); CPCM = CH_2Cl_2).

λ, nm		**Excitation**	**Assignation**
Observed (ε, x10^3 $M^{-1}cm^{-1}$)	**Calculated** (Osc. Strength)		
627 (52)	587 (0.889)	H -> L (99%)	Periphery -> Dist_2 + ADPM
414 (10)	452 (0.147)	H-1 -> L (93%)	Dist_2 -> Periphery + ADPM
	400 (0.283)	H-2 -> L (96%)	Side 1 -> Side 2 + ADPM
322 (40)	345 (0.505)	H-3 -> L (88%)	Prox 1+2 -> Dist 1+2 + ADPM
	337 (0.022)	H-11 (51%), H-10 (16%), H-6 (14%) -> L	Dist 1+2 -> Prox 1+2 + ADPM
	303 (0.050)	H-4 -> L (66%)	Periphery -> Dist_1 + ADPM
	292 (0.098)	H-12 -> L (47%); H -> L+1 (15%)	Periphery -> Prox_1 + ADPM
	290 (0.450)	H -> L+1 (67%); H-5 -> L (16%)	ADPM + Periphery -> Prox_1
	287 (0.063)	H-5 (64%), H-6 (10%) -> L (47%);	Dist 1+2 -> Prox 1+2 + ADPM
	283 (0.169)	H -> L+2 (42%); H-7 -> L (30%)	Periphery -> Dist_2 + ADPM

Figure S.32 – Experimental absorption spectrum in CH_2Cl_2 vs calculated optical absorption bands of ADPM **8** based on TD-DFT calculations (TD-BMK/6-311+G(2d,p); CPCM = CH_2Cl_2).

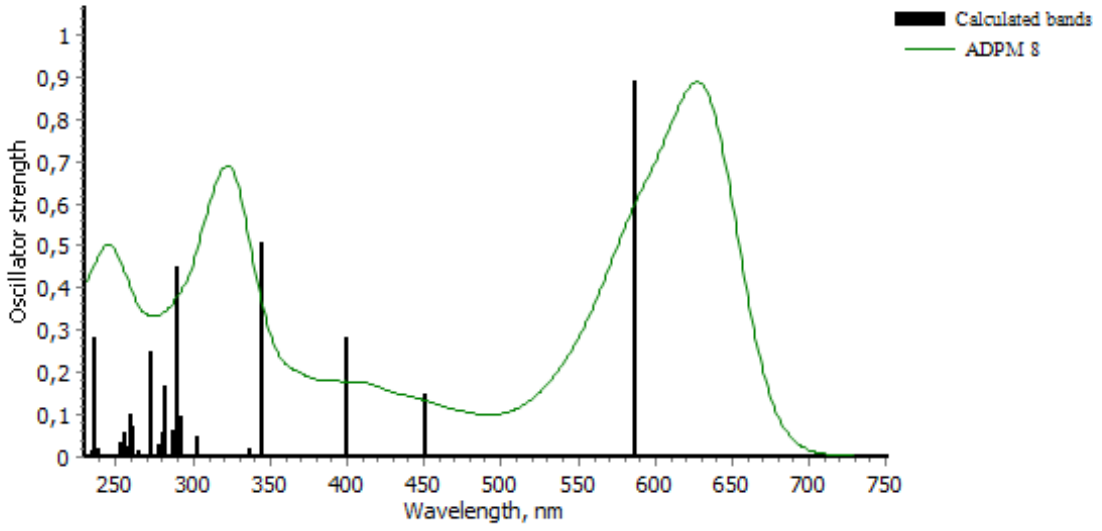

X-ray diffraction measurements and structure determination

Crystallographic data for **3** and **5** were collected at 150 K, from single crystal samples, which were mounted on a loop fiber. Data were collected using a Bruker Microstar diffractometer equipped with a Platinum 135 CCD Detector, a Helios optics and a Kappa goniometer. The crystal-to-detector distance was 3.8 cm, and the data collection was carried out in 512 x 512 pixel mode. The initial unit cell parameters were determined by a least-squares fit of the angular setting of strong reflections, collected by a 110.0 degree scan in 110 frames over three different parts of the reciprocal space. Crystallographic data for **1** and **4** were collected at 100 K, using a Bruker smart diffractometer equipped with an APEX II CCD Detector, a Incoatec IMuS source and a Quazar MX mirror. The crystal-to-detector distance was 4.0 cm, and the data collection was carried out in 512 x 512 pixel mode. The initial unit cell parameters were determined by a least-squares fit of the angular setting of strong reflections, collected by a 180.0 degree scan in 180 frames over three different parts of the reciprocal space. For determination of cell parameters, cell refinement and data reduction APEX2 was used.[1] Absorption corrections were applied using SADABS.[2] Structure solution was performed using direct methods with SHELXS97 and refined on F^2 by full-matrix least squares using SHELXL97.[3]

For **1**, **4** and **5**, all non-H atoms were refined by full-matrix least-squares with anisotropic displacement parameters. The H-atoms were included in calculated positions and treated as riding atoms: aromatic C—H 0.95 Å, methyl C—H 0.98 Å, with $U_{iso}(H) = k \times U_{eq}$ (parent C-atom), where k = 1.2 for the aromatic H-atoms and 1.5 for the methyl H-atoms. The H-atoms connected to heteroatoms (N and O) were in all cases located from the difference Fourier map. For **1** and **5**, they were freely refined. For **4**, in order to better model the disorder, the H-atoms on N and O

atoms were refined using the riding model, with appropriate thermal displacement coefficient: $U_{iso}(H) = 1.2 \times U_{eq}$(heteroatom).

The structure of the compound **3** was obtained from the best available crystal, which unfortunately was very poor quality, resulting in poor data quality. In addition, the whole molecule presents a very high degree of disorder. Therefore, only the isotropic refinement of the atoms was possible. All the H-atoms were located using the riding model. Under these circumstances, only the connectivity of the atoms can be discussed in this structure. The position of the pyridyl groups can be either *endo-* or *exo-*, but a final conclusion can't be derived from the analysis due to a so highly disordered model. The identity of the compound was confirmed by mass spectrometry performed on the same crystal sample (see experimental section).

For compound **4**, a very good data set was obtained, but nevertheless high residual electron density peaks were located during the refinement. They were considered to be highly disordered solvent molecules. All the attempts to model the solvent molecules were unsuccessful, and they were removed using the SQUEEZE routine from PLATON.[4] As a result, an improvement of the R_1 factor with ~ 2.3% was obtained. Solvent accessible voids of 56 $Å^3$ were found, containing 12 electrons. Water didn't fit. The structure of **4** contains 4 molecules in the asymmetric unit, and two of these display disorder at the level of the ADPM moiety and of the proximal phenyl groups, over two positions. The disorder was modelled as two components using PART instructions. The occupation factor was first refined, and then fixed at the values obtained after refinement [0.63:0.37]. The model was refined anisotropically. SIMU restraints were used.

The following software were used to prepare material for publication: PLATON, UdMX and Mercury.[4, 5, 6]. Figures were generated using ORTEP3 and POV-Ray.[7] Data were deposited in

CCDC under the deposit numbers: CCDC 1005388-1005391.[8] The alerts given by the checkCIF/ PLATON routine are commented in the crystallographic information files (cifs) of the corresponding compounds.

Table S.1 - Solid-state structure and refinement data for compounds **1**, **3**, **4** and **5**.

		1	**3**[a]	**4**[b]	**5**
Formula		C34 H27 N3	C30 H21 N5	C33 H25 N3 O2	C32 H24 N4 O
M_w(g/mol)		509.58	451.52	495.56	480.55
T (K)		100	150	100	100
Wavelength (Å)		1.54178	1.54178	1.54178	1.54178
Crystal System		Monoclinic	Monoclinic	Monoclinic	Monoclinic
Space Group		$P2_1/n$	$P2_1$	Pc	$P2_1/c$
Unit Cell:	a (Å)	14.2562(1)	5.6755(2)	20.1555(2)	11.3385(6)
	b (Å)	14.1356(1)	11.9628(4)	9.6757(1)	13.9762(7)
	c (Å)	14.3787(1)	16.5633(6)	25.4600(3)	15.3735(8)
	α (°)	90	90	90	90
	β (°)	117.825(1)	91.632(2)	100.668(1)	97.732(2)
	γ (°)	90	90	90	90
	V (Å^3)	2562.57(3)	1124.11(7)	4879.35(9)	2414.1(2)
Z		4	2	8	4
$d_{calcd.}$ (g/cm^3)		1.321	1.334	1.349	1.322
μ (mm^{-1})		0.656	0.636	0.674	0.644
F(000)		1072	472	2080	1008
θ range (°)		3.61 to 71.04	2.67 to 69.58	2.23 to 71.12	3.93 to 69.67
Reflections collected		100228	22472	94028	64766
Independent reflections		4923	4153	18292	4534
GoF		1.057	1.034	1.034	1.019
R1(F); wR(F^2) [I > 2σ(I)]		0.0360; 0.0883	0.1790; 0.3067	0.0461; 0.1183	0.0360; 0.0955
R1(F); wR(F^2) (all data)		0.0362; 0.0884	0.1853; 0.3091	0.0531; 0.1241	0.0390; 0.0984
Largest diff. peak and hole (e/Å^3)		0.256 and - 0.154	1.400 and - 0.653	0.306 and - 0.232	0.212 and - 0.191

[a] only isotropic refinement of the structure was possible due to a whole molecule disorder situation and poor quality of the crystal; we only aim to highlight the connectivity of the atoms in this structure.
[b] the SQUEEZE routine from PLATON was applied in the case of this structure (see text).

Table S.11 - Selected bond lengths (Å) and angles (°) for compounds **1**, **4** and **5**.

	1	**4**[a]	**5**
Bond length (Å)/ Angle (°)			
N1-C1	1.380(1)	1.392(8)[a]	1.384(1)
C1-N2	1.339(1)	1.332(8)[a]	1.342(1)
N2-C17	1.317(2)	1.320(7)[a]	1.318(2)
C17-N3	1.390(1)	1.400(7)[a]	1.391(2)
N1-C1-N2	125.6(1)	129.6(7)[a]	126.4(1)
C1-N2-C17	124.2(1)	129.2(7)[a]	123.0(1)
N2-C17-N3	126.6(1)	128.3(7)[a]	125.0(1)
Tilt angles (°) between the planes of the two central pyrrolic rings			
	10.9(1)	8.0(1)[b]	9.8(1)
Tilt angles (°) between ADPM moiety and the aryl rings[c]			
Ar_1 (proximal)	13.6(1)	1.2(1) - 2.4(1)[b]	17.5(1)
Ar_2 (distal)	9.5(1)	28.7(1) - 38.1(1)[b]	35.7(1)
Ar_3 (distal)	45.3(1)	24.8(1) - 38.2(1)[b]	27.5(1)
Ar_4 (proximal)	26.4(1)	1.2(1) - 4.2(1)[b]	19.8(1)

[a] average values on the four molecules in the asymmetric unit; the error was calculated using the formula for propagation of error in calculations.
[b] values are shown as range for the four molecules in the asymmetric unit.
[c] see Figure 1 in the article for the numbering of the aryl rings.

Table S.12 – Intramolecular H-bonding for compounds **1**, **4** and **5**. Distances are in Å and angles in degree (°). 3-center bifurcated H-bonds are displayed in *italic*.

D*—H···*A	***D*—H**	**H···*A***	***D*···*A***	***D*—H···*A***
1				
N1—H1···N3	*0.88(1)*	*2.16(1)*	*2.76(1)*	*125(1)*
N1—H1···O1	*0.88(1)*	*2.12(1)*	*2.64(1)*	*117(1)*
C10—H10···N2	0.95(1)	2.31(1)	2.99(1)	129(1)
C19—H19···O2	0.95(1)	2.41(1)	2.87(1)	109(1)
C32—H32···N3	0.95(1)	2.46(1)	2.80(1)	101(1)
4 (values are shown for one of the 4 molecules in the asymmetric unit; similar intramolecular H-bonding pattern is observed for the other three molecules)				
N1—H1A···O1	*0.86(1)*	*2.20(1)*	*2.73(1)*	*120(1)*
N1—H1···N3	*0.86(1)*	*2.59(1)*	*3.06(1)*	*116(1)*
O2—H2B···N3	0.82(1)	1.88(1)	2.60(1)	146(1)
C6—H6···N2	0.93(1)	2.53(1)	3.05(1)	116(1)
C26—H26···N2	0.93(1)	2.46(1)	3.03(1)	119(1)
5				
N1—H1···N3	*0.88(1)*	*2.19(1)*	*2.70(1)*	*124(1)*
N1—H1···O1	*0.88(1)*	*2.15(1)*	*2.65(1)*	*116(1)*
C6—H6···N2	0.95(1)	2.62(1)	3.10 (1)	112(1)
C22—H22···N2	0.95(1)	2.48(1)	3.05(1)	118(1)

Figure S.33 – Packing diagram for compound **4**: space-filling model showing the π – π and π – H-C(sp^2) intermolecular interactions.

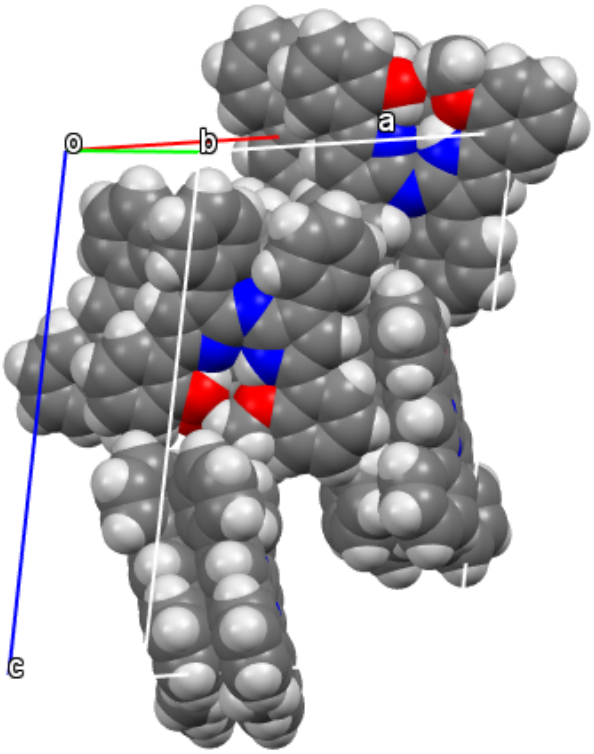

References

1. *APEX2, Bruker AXS*, Madison, WI 53719-1173, 2009-2013.
2. Sheldrick, G. M. *SADABS*, 1996.
3. *SHELXTL, Bruker AXS* Madison, WI 53719-1173, 2001.
4. Spek, A. L. *PLATON*, 2003.
5. Maris, T. *UdMX*, 2004-2013.
6. CCDC *Mercury 3.1*, 2001-2012.
7. (a) Farrugia, L. J., ORTEP-3 for windows - a version of ORTEP-III with a graphical user interface (GUI). *J. Appl. Crystallogr.* **1997,** *30* (Copyright (C) 2012 American Chemical Society (ACS). All Rights Reserved.), 565; (b) *POV-Ray* Persistence of Vision Pty. Ltd., retrieved from http://www.povray.org/download/: 2004.
8. CCDC 1005388-1005391 contains the supplementary crystallographic data for this paper. These data can be obtained free of charge via http://www.ccdc.cam.ac.uk/data_request/cif, or by emailing data_request@ccdc.cam.ac.uk, or by contacting The Cambridge Crystallographic Data Centre, 12, Union Road, Cambridge CB2 1EZ, UK; fax: +44 1223 336033.